0.954, $P$ = 0.3443), but not effects of group, on latency, without a significant interaction (Figure 2a-c). The subsequent Student t test on the changes of P300 latency revealed no significant difference between two drugs (Figure 2g-i). With regard to amplitude, two-way repeated ANOVA indicated no significant effects of treatment without a significant interaction (Figure 2d-f, j-l).

### Effects of treatments with etizolam and ethyl loflazepate on neuropsychological tests

For acute effects of drug treatment on neuropsychological tests, two-way repeated ANOVA showed significant practice effects of repeated testing, but not effects of drug group, on test scoring without a significant interaction in some tests including trail making A (F (1,16) = 7.399, $P$ = 0.0151, Figure 3a), trail making B (F (1,16) = 8.409, $P$ = 0.0104, Figure 3b), digit span forward (F (1,16) = 8.696, $P$ = 0.0094, Figure 3c), verbal paired associates immediate memory (F(1,16) = 6.485, $P$ = 0.0215, Figure 3e) and digit symbol (F(1,16) = 24.209, $P$ = 0.0002, Figure 3g), and no significant effects of repeated testing and drugs on test scoring without a significant interaction in other tests such as digit span backward (Figure 3d) and verbal paired associates delayed recall (Figure 3f).

For subchronic effects of drug treatment on neuropsychological tests, two-way repeated ANOVA indicated significant practice effects of repeated testing, but not effects of drug group, on test scoring without a significant interaction, in some tests including trail making test A (F (1,15) = 12.472, $P$ = 0.0030, Figure 3h), trail making test B (F (1,15) = 5.426, $P$ = 0.0342, Figure 3i), digit span forward (F (1,15) = 7.092, $P$ = 0.0177, Figure 3j), verbal paired associates immediate memory (F (1,15) = 16.449, $P$ = 0.0010, Figure 3l), verbal paired associates delayed recall (F (1,15) = 5.773, $P$ = 0.0297, Figure 3m) and digit symbol (F (1,15) = 6.075, $P$ = 0.0236, Figure 3n), and no significant effects of repeated testing and drug group on test scoring without a significant interaction in digit span backward test (Figure 3k).

## Discussion

Our results show acute drug treatment induced prolongation in P300 latency. This is consistent with previous studies demonstrating that benzodiazepines such as alprazolam, lorazepam, clonazepam and triazolam induce prolongation in P300 latency [6,16,18,19]. However, subsequent ANOVA revealed that etizolam (1 and 2 mg) induced significant prolongation in P300 latency compared to ethyl loflazepate (1 mg). The difference

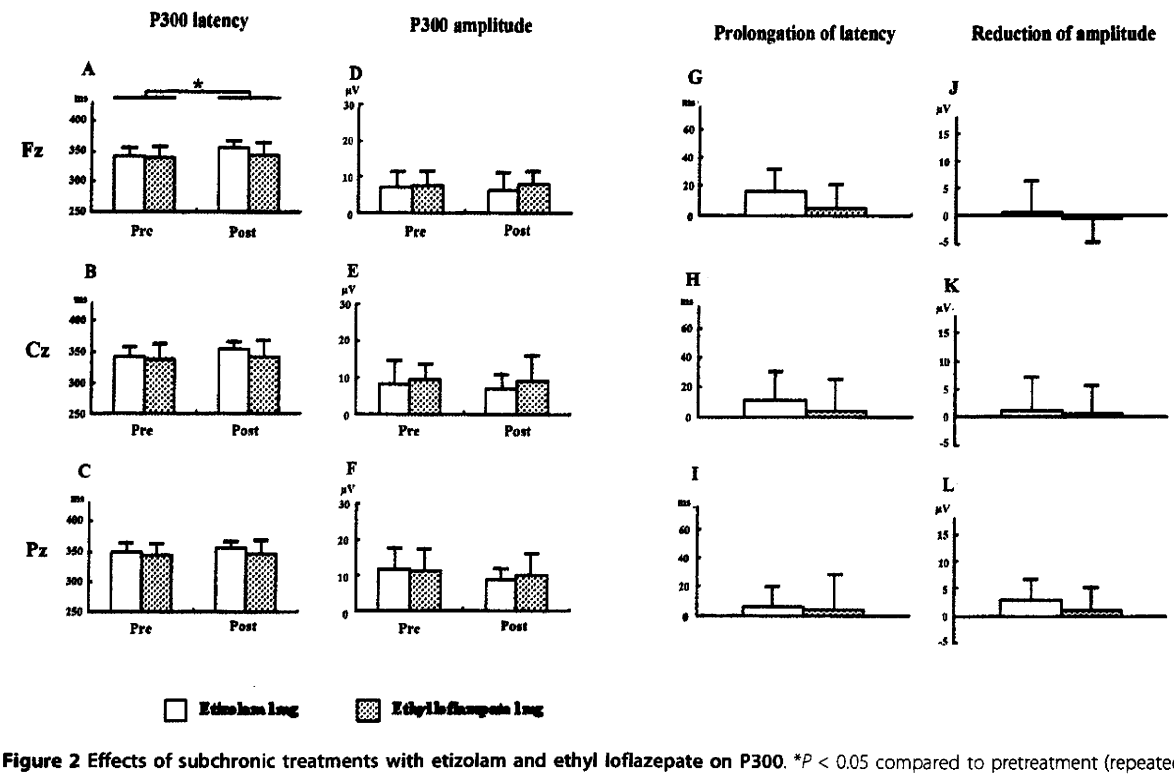


**Figure 2 Effects of subchronic treatments with etizolam and ethyl loflazepate on P300.** *$P$ < 0.05 compared to pretreatment (repeated analysis of variance (ANOVA)).

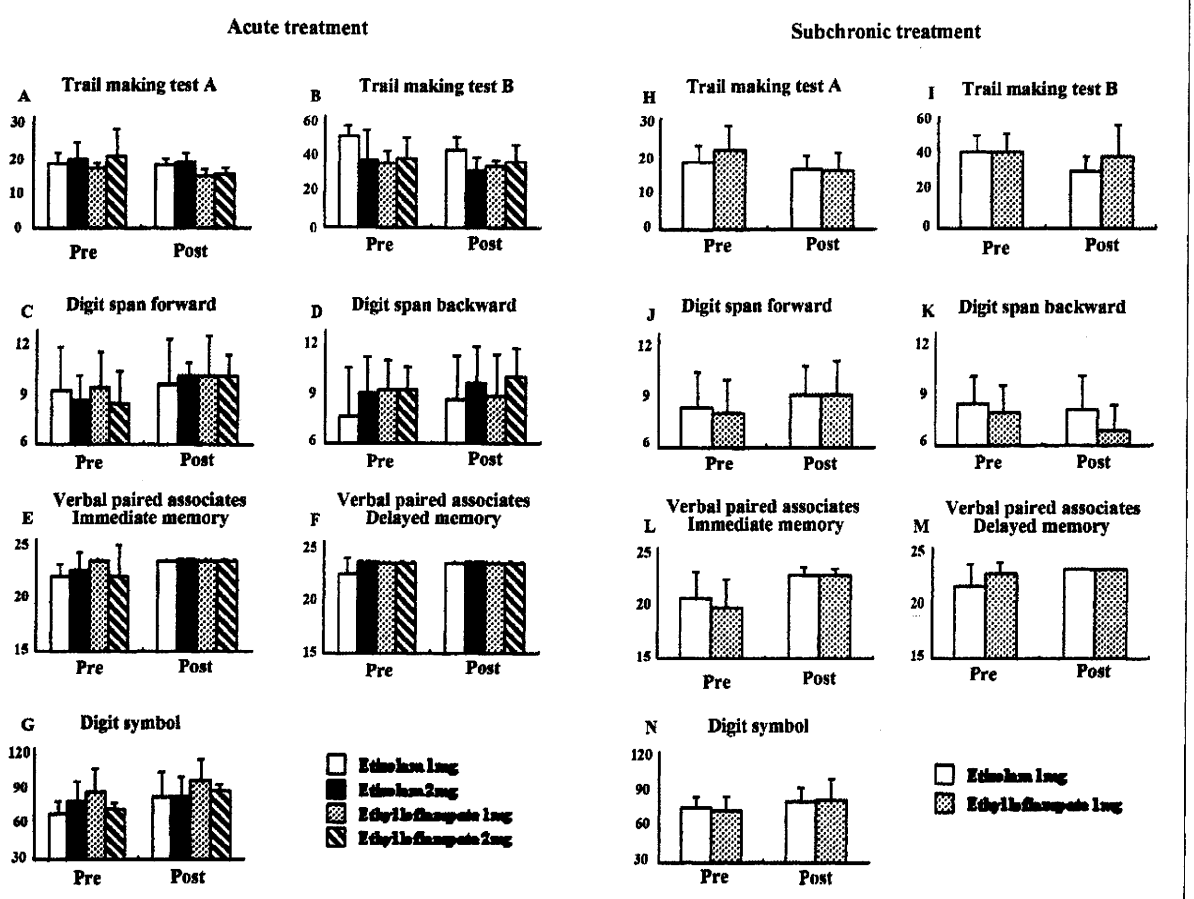


**Figure 3** Effects of acute and subchronic treatment with etizolam and ethyl loflazepate on neuropsychological tests.

between the acute effects of etizolam and ethyl loflazepate could contribute to the potent sedative effects of etizolam, although equivalent doses of these two drugs to diazepam are clinically almost the same. P300 latency is suggested to reflect the stimulus evaluation time, and is relatively independent of response selection and execution [28-30]. Therefore, it is conceivable that ethyl loflazepate has less effect on P300-related information processing, although the subjects did not exhibit any harmful effects on motor skills, visuomotor tracking speed, and delayed memory in the neuropsychological tests.

Secondly, subchronic treatment with drugs produced prolongation in P300 latency only in the Fz regions. Weak prolongation in P300 latency was seen in the etizolam-treated subjects (although this was not statistically significant). The magnitude of prolongation by subchronic ethizolam treatment was reduced when compared to the acute administration of etizolam. In support of this finding, previous studies reported that people develop tolerance to the sedative and cognitive effects of benzodiazepines after subchronic treatments [1]. Interestingly, subchronic treatment of ethyl loflazepate did not prolong the latency in spite of its long elimination rate.

Finally, acute but not subchronic treatment with benzodiazepine reduced P300 amplitude. Based on the magnitude of changes, the main effects on the reduction of P300 amplitude were produced by etizolam (2 mg). This result replicated previous studies that benzodiazepine anxiolytic drugs (lorazepam, clonazepam and alprazolam) induced reductions in P300 amplitude [15,17]. Recent studies demonstrated that reduction in auditory P300 amplitude correlated with the severity of thought disorders [31,32]. Previous studies reported that a single administration of a benzodiazepine drug produced impairment of learning and memory [1-3]. However, the present study showed no aversive effects of the examined drugs on neuropsychological tasks such as attention-needed tasks (trails making test, digit span) and memory (verbal paired associates, digit symbol). Since the subjects were free from abnormal pathological

process, alterations in the P300 may be induced by etizolam, not by symptom alleviation due to etizolam.

Differences in the effects on P300 latency between etizolam and ethyl loflazepate could be attributed to their pharmacological properties, such as sedative effects, and affinities for ω-1 and ω-2 sites. Etizolam is short acting (EH of 6 h) whereas ethyl loflazepate is long acting (EH of 122 h).

With regard to limitations of the present study, the sample size was small.

## Conclusions

Acute administration of etizolam induced significant prolongation in P300 latency whereas low dose ethyl loflazepate induced fewer effects on P300 latency in the Fz, Cz and Pz regions than low-dose etizolam. For a while, subchronic administration of etizolam, but not ethyl loflazepate, caused weak prolongation in P300 latency in the Fz but not Cz and Pz regions. In contrast, acute and chronic administrations of etizolam and ethyl loflazepate showed no deficits in motor skills, visuomotor tracking speed, and delayed memory on neuropsychological testing.

**Author details**
[1]Department of Psychiatry, Chiba University Graduate School of Medicine, Chiba, Japan. [2]Division of Clinical Neuroscience, Chiba University Center for Forensic Mental Health, Chiba, Japan.

**Authors' contributions**
GF conceived the paper, designed the study, performed the psychological measures, collected data, carried out the statistical analysis and drafted the paper; THash performed the psychological measures; YS carried out the statistical analysis and helped draft the study; THase, HW and MF supervised the study; KH and MI designed the study and helped draft the papers. All authors read and approved the final manuscript.

**Competing interests**
The authors declare that they have no competing interests.

Received: 13 June 2010 Accepted: 3 November 2010
Published: 3 November 2010

**References**

1. Files SE, Lister RG: **Lorazepam-induced deficits in learning result from impaired rehearsal, reduced motivation, or increased sedation?** *Br J Clin Pharmacol* 1982, **14**:545-550.
2. Block RI, Berchou R: **Alprazolam and lorazepam effects on memory acquisition and retrieval processes.** *Pharmac Biochem Behav* 1984, **20**:233-241.
3. Curran HV: **Tranquilizing memories: a review of the effects of benzodiazepines on human memory.** *Biol Psychology* 1986, **23**:179-213.
4. Chouinard GJ: **Issues in the clinical use of benzodiazepines: potency, withdrawal, and rebound.** *J Clin Psychiatry* 2004, **65(Suppl 5)**:7-12.
5. Stewart SA: **The effects of benzodiazepines on cognition.** *J Clin Psychiatry* 2005, **66(Suppl 2)**:9-13.
6. Urata J, Uchiyama M, Iyo M, Enomoto T, Hayakawa T, Tomiyama M, Nkajima T, Sasaki H, Shirakawa S, Wada K, Fukui S, Yamadera H, Okawa M: **Effects of a small dose of triazolam on P300 and resting EEG.** *Psychopharmacology* 1996, **125**:179-184.
7. Polich J, Kok A: **Cognitive and biological determinants of P300: an integrative review.** *Biol Psychology* 1995, **41**:103-146.
8. Emmerson RY, Dustman RE, Shearer DE, Turner CW: **P3 latency and symbol digit performance correlations in aging.** *Exp Aging Res* 1989, **15**:151-159.
9. O'Donell BF, Friedman S, Swearer JM, Drachman DA: **Active and passive P3 latency and psychometric performance: influence of age and individual differences.** *Int J Psychophysiol* 1992, **12**:187-195.
10. Knight RT, Scabini D: **Anatomic bases of event-related potentials and their relationship to novelty detection in humans.** *J Clin Neurophysiol* 1998, **15**:3-13.
11. Fjell AM, Walhovd KB: **P300 and neuropsychological tests as measures of aging: salp topography and cognitive changes.** *Brain Topogr* 2001, **14**:25-40.
12. McAllister-Williams RH, Massey AE, Rugg MD: **Effects of tryptophan depletion on brain potential correlates of episodic memory retrieval.** *Psychopharmacology* 2002, **160**:434-442.
13. Walhoved KB, Fjell AM: **The relationship between P3 and neuropsychological function in an adult life span sample.** *Biol Psychology* 2003, **62**:65-87.
14. Pogarell O, Mulert C, Hegerl U: **Event related potentials and fMRI in neuropsychopharmacology.** *Clin EEG Neurosci* 2006, **37**:99-107.
15. Berchou R, Chiyasirisobhon S, Green V, Mason K: **The pharmacodynamic properties of lorazepam and methylphenidate drugs on event-related potentials and power spectral analysis in normal subjects.** *Clin Electroencephalogr* 1986, **17**:176-180.
16. Shinotoh H, Iyo M, Yamada T, Inoue O, Suzuki K, Itoh T, Fukuda H, Yamasaki T, Tateno Y, Hirayama K: **Detection of benzodiazepine receptor occupancy in the human brain by positron emission tomography.** *Psychopharmacology* 1989, **99**:202-207.
17. Rockstroh B, Elbert T, Lutzenberger W, Altenmuller E: **Effects of the anticonvulsant benzodiazepine clonazepam on event-related brain potentials in humans.** *Electroencephalogr Clin Neurophysiol* 1991, **78**:142-149.
18. Semlitsch HV, Anderer P, Saletu B: **Acute effects of the anxiolytics suriclone and alprazolam on cognitive information processing utilizing topographic mapping of event-related brain potentials (P300) in healthy subjects.** *Eur J Clin Pharmacol* 1995, **49**:183-191.
19. Nichols JM, Martin F: **The effect of lorazepam on memory and event-related potentials in heavy and light social drinkers.** *Psychophysiology* 1996, **33**:446-456.
20. Hayakawa T, Uchikawa M, Urata J, Enomoto T, Okubo J, Okawa M: **Effects of small dose of triazolam on P300.** *Psychiatry Clin Neurosci* 1999, **53**:185-187.
21. Chambon JP, Perio A, Demarne H, Hallot A, Dantzer R, Roncucci R, Biziere K: **Ethyl loflazepate: a prodrug from the benzodiazepine series designed to dissociate anxiolytic and sedative activities.** *Arzneimittelforschung* 1985, **35**:1573-1577.
22. Tsumagari T, Nakajima A, Fukuda T, Shuto S, Kenjo T, Morimoto Y, Takigawa Y: **Pharmacological properties of 6-(o-chlorophenyl)-8-ethyl-1-methyl-4H-s-triazolo[3,4-c]thieno[2,3-e] [1,4]diazepine (Y-7131), a new anti-anxiety drug.** *Arzneimittelforschung* 1978, **28**:1158-64.
23. Inagaki A, Inada T, Fujii Y, Yagi K, Yoshio T, Nakamura H, Yamauchi T: *Dose equivalence of psychotropic drugs [in Japanese]* Tokyo, Japan: Seiwa Shoten Co. Ltd; 1999, 99-121.
24. Inada T, Nozaki S, Inagaki A, Furukawa TA: **Efficacy of diazepam as an anti-anxiety agent: meta-analysis of double-blind, randomized controlled trials carried out in Japan.** *Human Psychopharmac Clin Exp* 2003, **18**:483-487.
25. Reitan RM, Wolfson D: *The Halstead-Reitan Neuropsychological Test Battery* Tucson, AZ, USA: Neuropsychology Press; 1985.
26. Smith A: *Symbol Digit Modalities Test (SDMT): Manual (revised)* Los Angeles, CA, USA: Western Psychological Services; 1982.
27. Wechsler DA: *Wechsler Memory Scale-Revised, Manual* New York, USA: Psychological Corp; 1987.
28. Kutas M, McCarthy G, Donchin E: **Augmenting mental chronometry: the P300 as a measure of stimulus evaluation time.** *Science* 1977, **197**:792-795.
29. McCarthy G, Donchin E: **A metric for thought: a comparison of P300 latency and reaction time.** *Science* 1981, **211**:77-80.
30. Magliero A, Bashoe TR, Coles MG, Donchin E: **On the dependence of P300 latency on stimulus evaluation processes.** *Psychophysiology* 1984, **21**:171-186.

31. Higashima M, Nagasawa T, Kawasaki Y, Oka T, Sakai N, Tsukada T, Koshino Y: **Auditory P300 amplitude as a state marker for positive symptoms in schizophrenia: cross-sectional and retrospective longitudinal studies.** *Schizophr Res* 2001, **59**:147-157.
32. Iwanami A, Okajima Y, Isono H, Shinoda J, Kasai K, Hata A, Fukuda M, Nakagome K, Kamijima K: **Effects of risperidone on event-related potential in schizophrenic patients.** *Pharmacopsychiatry* 2001, **34**:73-79.

doi:10.1186/1744-859X-9-37
**Cite this article as:** Fukami *et al.*: Effects of etizolam and ethyl loflazepate on the P300 event-related potential in healthy subjects. *Annals of General Psychiatry* 2010 **9**:37.

OPEN ACCESS Freely available online

PLoS one

# Essential Role of NMDA Receptor Channel ε4 Subunit (GluN2D) in the Effects of Phencyclidine, but Not Methamphetamine

**Yoko Hagino[1], Shinya Kasai[1], Wenhua Han[1], Hideko Yamamoto[1], Toshitaka Nabeshima[2], Masayoshi Mishina[3], Kazutaka Ikeda[1]***

**1** Division of Psychobiology, Tokyo Institute of Psychiatry, Tokyo, Japan, **2** Comparative Cognitive Science Institutes and Department of Chemical Pharmacology, Graduate School of Pharmaceutical Sciences, Meijo University, Nagoya, Japan, **3** Department of Molecular Neurobiology and Pharmacology, Graduate School of Medicine, The University of Tokyo, Tokyo, Japan

## Abstract

Phencyclidine (PCP), a noncompetitive *N*-methyl-D-aspartate (NMDA) receptor antagonist, increases locomotor activity in rodents and causes schizophrenia-like symptoms in humans. Although activation of the dopamine (DA) pathway is hypothesized to mediate these effects of PCP, the precise mechanisms by which PCP induces its effects remain to be elucidated. The present study investigated the effect of PCP on extracellular levels of DA ($DA_{ex}$) in the striatum and prefrontal cortex (PFC) using *in vivo* microdialysis in mice lacking the NMDA receptor channel ε1 or ε4 subunit (GluRε1 [GluN2A] or GluRε4 [GluN2D]) and locomotor activity. PCP significantly increased $DA_{ex}$ in wildtype and GluRε1 knockout mice, but not in GluRε4 knockout mice, in the striatum and PFC. Acute and repeated administration of PCP did not increase locomotor activity in GluRε4 knockout mice. The present results suggest that PCP enhances dopaminergic transmission and increases locomotor activity by acting at GluRε4.

**Citation:** Hagino Y, Kasai S, Han W, Yamamoto H, Nabeshima T, et al. (2010) Essential Role of NMDA Receptor Channel ε4 Subunit (GluN2D) in the Effects of Phencyclidine, but Not Methamphetamine. PLoS ONE 5(10): e13722. doi:10.1371/journal.pone.0013722

**Editor:** Kenji Hashimoto, Chiba University Center for Forensic Mental Health, Japan

**Received** July 2, 2010; **Accepted** October 5, 2010; **Published** October 28, 2010



**Funding:** This work was supported by grants from the Ministry of Health, Labour and Welfare of Japan (H19-Iyaku-023, H22-Iyaku-015), the Ministry of Education, Culture, Sports, Science and Technology of Japan, The Naito Foundation, and The Mitsubishi Foundation. The funders had no role in study design, data collection and analysis, decision to publish, or preparation of the manuscript.

**Competing Interests:** The authors have declared that no competing interests exist.

* E-mail: ikeda-kz@igakuken.or.jp

## Introduction

Phencyclidine (PCP) is a drug of abuse that causes psychosis resembling both the positive (e.g., hallucinations, paranoia) and negative (e.g., emotional withdrawal, motor retardation) signs of schizophrenia in humans [1]. Acute administration of PCP to rodents produces increases in locomotor activity, stereotypy, and ataxia [2,3]. Repeated PCP administration produces sensitization of locomotor activity, rearing, and stereotypy but tolerance to ataxia [3–5]. PCP acts as a noncompetitive antagonist of the *N*-methyl-D-aspartate (NMDA) excitatory amino acid receptor [6–8]. Additionally, high doses of PCP block dopamine (DA) reuptake [1,9–11]. Similar to PCP, amphetamine (AMPH) and its derivative methamphetamine (METH) produce behavioral sensitization to locomotor activity, rearing, and stereotypy when they are repeatedly administered [12,13]. Amphetamine and METH facilitate dopaminergic neurotransmission via a number of mechanisms [14], including DA efflux by reverse transport through the dopamine transporter (DAT) [15–18], inhibition of DA uptake [19–21], and inhibition of monoamine oxidase (MAO) activity [22–24].

The NMDA receptor channel subunit family is composed of seven subunits—GluRζ (GluN1), GluRε1-4 (GluN2A-D), and GluRχ1, 2 (GluN3A, B)—which are all products of separate genes [25]. In the rodent and human brains, GluRε1 and GluRε2 are predominant subunits expressed in the forebrain. GluRε3 is expressed largely in cerebellar granule cells and selectively in several other brain regions. GluRε4 is expressed in the diencephalon and midbrain and is more prominent during early development [26]. Highly active NMDA receptor channels are produced when the GluRζ subunit is expressed together with one of the four GluRε subunits in *Xenopus* oocytes and mammalian cells [27–30]. Four GluRε subunits are major determinants of the functional properties of NMDA receptor channels [31]. Noncompetitive NMDA receptor antagonists (i.e., PCP, ketamine, and SKF-10,047) block the four GluRε/GluRζ channels to similar extents in *Xenopus* oocytes [32]. Gene-targeting techniques provide an efficient method for clarifying the distinct functions of these NMDA receptor channel subunits. GluRε1 knockout mice display increased locomotor activity, whereas GluRε4 knockout mice exhibit reduced locomotor activity in a novel environment [33–36]. GluRε3 knockout mice show few apparent deficits [37–39]. Investigating the physiological functions of GluRζ or GluRε2 knockout mice, in contrast, is nearly impossible because these two mutants die shortly after birth [40–42].

To clarify the contributions of NMDA receptor channel subunits in the PCP-induced increases in extracellular levels of dopamine ($DA_{ex}$) and locomotor responses, we investigated the effects of METH and PCP on $DA_{ex}$ in the striatum and prefrontal cortex (PFC) using *in vivo* microdialysis and measuring locomotor activity in GluRε1 knockout (GluRε1$^{-/-}$) and GluRε4 knockout (GluRε4$^{-/-}$) mice.

## Results

### Baseline $DA_{ex}$ in the striatum and PFC in GluRε1$^{-/-}$ and GluRε4$^{-/-}$ mice

Baseline $DA_{ex}$ was not different between wildtype, GluRε1$^{-/-}$, and GluRε4$^{-/-}$ mice in the striatum (one-way analysis of variance [ANOVA]: $F_{2,67}=0.412$, $p=0.664$) and PFC (one-way ANOVA: $F_{2,59}=1.025$, $p=0.365$). Mean baseline $DA_{ex}$ in the striatum was 51.89±3.57 fmol/10 µl ($n=27$) for wildtype, 49.35±5.35 fmol/10 µl ($n=19$) for GluRε1$^{-/-}$, and 46.75±3.93 fmol/10 µl ($n=24$) for GluRε4$^{-/-}$ mice. Mean baseline $DA_{ex}$ in the PFC was 1.29±0.20 fmol/10 µl ($n=23$) for wildtype, 1.59±0.30 fmol/10 µl ($n=20$) for GluRε1$^{-/-}$, and 1.10±0.21 fmol/10 µl ($n=19$) for GluRε4$^{-/-}$ mice.

### Effects of acute METH administration on $DA_{ex}$ in the striatum and PFC in GluRε1$^{-/-}$ and GluRε4$^{-/-}$ mice

Methamphetamine (1 mg/kg) markedly increased $DA_{ex}$ in the striatum and PFC in wildtype, GluRε1$^{-/-}$, and GluRε4$^{-/-}$ mice (Fig. 1A, C). Two-way ANOVA (drug × genotype) of $DA_{ex}$, measured as the area-under-the-curve (AUC) calculated during a 180 min posttreatment period, revealed a significant effect of drug ($F_{1,39}=47.418$, $p<0.001$) but not genotype ($F_{2,39}=0.889$, $p=0.419$) and no significant drug × genotype interaction ($F_{2,39}=0.739$, $p=0.484$) in the striatum (Fig. 1B). Similarly, in the PFC, two-way ANOVA (drug × genotype) of AUC values revealed a significant effect of drug ($F_{1,31}=48.784$, $p<0.001$) but not genotype ($F_{2,31}=0.320$, $p=0.728$) and no significant drug × genotype interaction ($F_{2,31}=0.201$, $p=0.819$) (Fig. 1B).

### Effects of acute PCP administration on $DA_{ex}$ in the striatum and PFC in GluRε1$^{-/-}$ and GluRε4$^{-/-}$ mice

Phencyclidine (3 mg/kg) markedly increased $DA_{ex}$ in wildtype and GluRε1$^{-/-}$ mice, but not in GluRε4$^{-/-}$ mice, in the striatum and PFC (Fig. 2A, C). Two-way ANOVA (drug × genotype) of AUC values revealed a significant effect of drug ($F_{1,39}=17.201$, $p<0.001$) but not genotype ($F_{2,39}=2.012$, $p=0.147$) in the striatum and a significant drug × genotype interaction ($F_{2,39}=3.314$, $p=0.047$) (Fig. 2B). *Post hoc* comparisons revealed that the effect of PCP on $DA_{ex}$ in GluRε4$^{-/-}$ mice was significantly less compared with wildtype and GluRε1$^{-/-}$ mice ($p=0.002$ and 0.03, respectively; Fisher's Protected Least Significant Difference [PLSD] *post hoc* test) in the striatum (Fig. 2B). In the PFC, two-way ANOVA (drug × genotype) of AUC values revealed a significant effect of drug ($F_{1,37}=35.215$, $p<0.001$) but not genotype ($F_{2,37}=1.969$, $p=0.154$) and a significant drug × genotype interaction ($F_{2,37}=3.326$, $p=0.047$) (Fig. 2D). *Post hoc* comparisons revealed that the effect of PCP on $DA_{ex}$ in GluRε4$^{-/-}$ mice was significantly less compared with wildtype and GluRε1$^{-/-}$ mice ($p=0.007$ and 0.003, respectively; Fisher's PLSD *post hoc* test) in the PFC (Fig. 2D).

### Locomotor activity in GluRε1$^{-/-}$ and GluRε4$^{-/-}$ mice in a novel environment

Locomotor activity in a novel environment was different between wildtype, GluRε1$^{-/-}$, and GluRε4$^{-/-}$ mice during the habituation period (mixed-design ANOVA: genotype, $F_{2,123}=35.423$, $p<0.0001$; time, $F_{2,123}=486.554$, $p<0.0001$; genotype × time, $F_{4,123}=15.337$, $p<0.0001$) (Fig. 3). Locomotor activity in a novel environment during the 60 min period increased in GluRε1$^{-/-}$ mice ($p=0.0002$, unpaired *t*-test) but decreased in GluRε4$^{-/-}$ mice ($p<0.0001$, Student's *t*-test) compared with wildtype mice. GluRε1$^{-/-}$ mice did not habituate during the 180 min period compared with wildtype mice ($p<0.0001$, Student's *t*-test).

### Effects of acute administration of METH and PCP on locomotor activity in GluRε1$^{-/-}$ and GluRε4$^{-/-}$ mice

Two-way ANOVA (drug × genotype) of locomotor activity data during the 60 min period revealed significant effects of drug

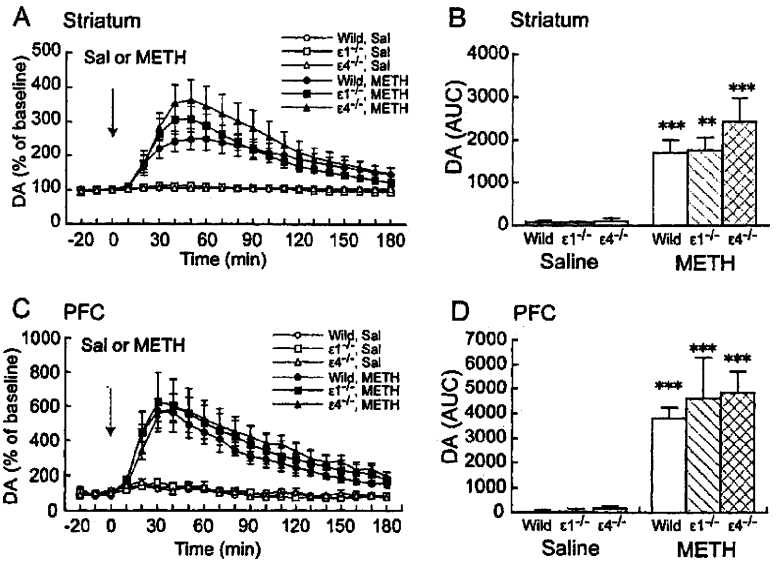


**Figure 1. Effects of acute METH on $DA_{ex}$ in the striatum and PFC in wildtype, GluRε1$^{-/-}$, and GluRε4$^{-/-}$ mice.** (**A, C**) Temporal pattern of $DA_{ex}$ before and after s.c. saline (Sal) or METH (1 mg/kg) injection. The arrows indicate the drug injection time. Each point represents the mean ± SEM of the percentage of $DA_{ex}$ baseline. (**B, D**) Histogram representing the mean AUC ± SEM of $DA_{ex}$ during the 180 min period after saline or METH injection ($n=5$–9). **$p<0.01$, ***$p<0.001$, compared with saline group of the same genotype (two-way ANOVA followed by Fisher's PLSD *post hoc* test).

doi:10.1371/journal.pone.0013722.g001

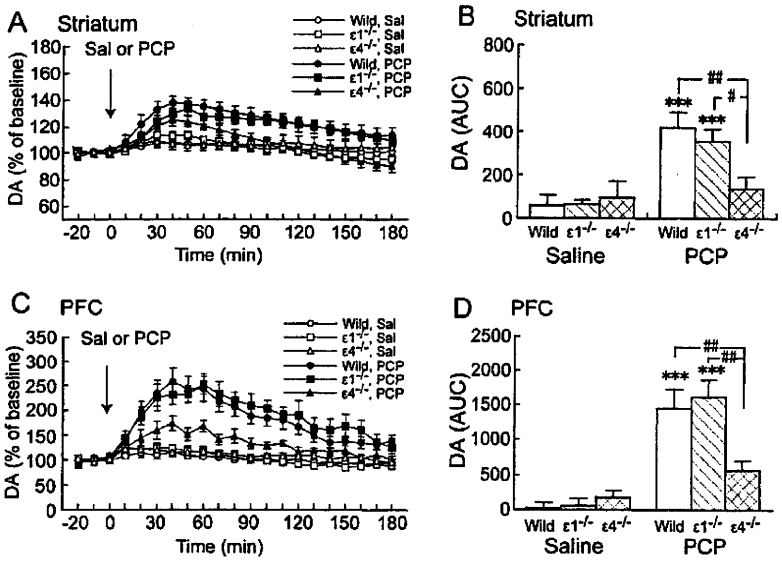


**Figure 2. Effects of acute PCP on $DA_{ex}$ in the striatum and PFC in wildtype, GluRε1$^{-/-}$, and GluRε4$^{-/-}$ mice.** (A, C) Temporal pattern of $DA_{ex}$ before and after s.c. saline (Sal) or PCP (3 mg/kg) injection. The arrows indicate the drug injection time. Each point represents the mean ± SEM of the percentage of $DA_{ex}$ baseline. (B, D) Histogram representing the mean AUC ± SEM of $DA_{ex}$ during the 180 min period after saline or PCP injection ($n$ = 5–11). ***$p$<0.001, compared with saline group of the same genotype; $^{\#}p$<0.05, $^{\#\#}p$<0.01, comparisons between genotypes in the same drug treatment (two-way ANOVA followed by Fisher's PLSD *post hoc* test).
doi:10.1371/journal.pone.0013722.g002

($F_{2,155}$ = 8.646, $p$ = 0.0002) and genotype ($F_{2,155}$ = 11.769, $p$<0.0001) and a significant drug × genotype interaction ($F_{4,155}$ = 5.734, $p$ = 0.0002) (Fig. 4). Methamphetamine (1 mg/kg) significantly increased locomotor activity during the 60 min period after the METH injection in wildtype mice ($p$ = 0.002, Student's $t$-test) and GluRε4$^{-/-}$ mice ($p$ = 0.0004, Student's $t$-test) compared with saline. However, METH (1 mg/kg) did not increase locomotor activity during the 60 min period after the METH injection in GluRε1$^{-/-}$ mice ($p$ = 0.411, Student's $t$-test) compared with saline.

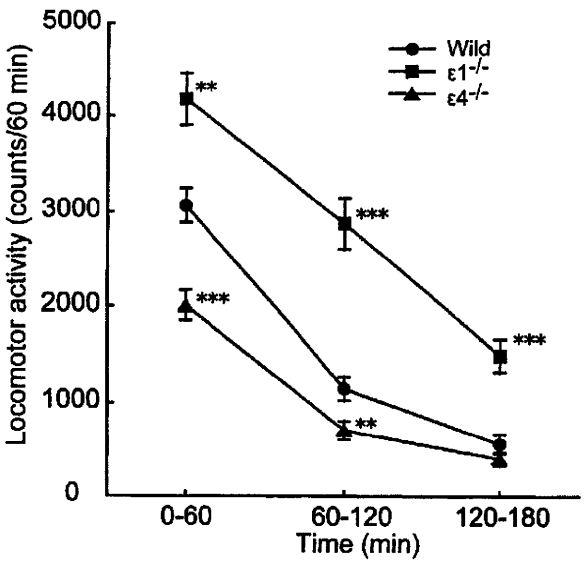


**Figure 3. Locomotor activity in wildtype, GluRε1$^{-/-}$, and GluRε4$^{-/-}$ mice in a novel environment.** Locomotor activity was measured for 180 min. Each point represents the mean ± SEM ($n$ = 34–50). *$p$<0.05, **$p$<0.01, ***$p$<0.001, compared with wildtype mice (one-way ANOVA followed by Fisher's PLSD *post hoc* test).
doi:10.1371/journal.pone.0013722.g003

Phencyclidine (3 mg/kg) significantly increased locomotor activity during the 60 min period after the PCP injection in wildtype mice ($p$ = 0.008, Student's $t$-test) and GluRε1$^{-/-}$ mice ($p$ = 0.045, Student's $t$-test) compared with saline treatment. However, PCP (3 mg/kg) did not increase locomotor activity in GluRε4$^{-/-}$ mice ($p$ = 0.142, unpaired $t$-test) compared with saline treatment.

## Effects of repeated administration of METH and PCP on locomotor activity in GluRε1$^{-/-}$ and GluRε4$^{-/-}$ mice

Mixed-design ANOVA of locomotor activity data during the 60 min period after the METH injection from Session 1 to 8 revealed significant effects of genotype ($F_{2,385}$ = 3.350, $p$ = 0.042) and session ($F_{7,385}$ = 16.091, $p$<0.0001) but no significant genotype × session interaction ($F_{14,385}$ = 0.611, $p$ = 0.857) (Fig. 5A). Chronic METH (1 mg/kg) injections increased locomotor activity in wildtype ($p$<0.0001, paired $t$-test), GluRε1$^{-/-}$ ($p$ = 0.0007, paired $t$-test), and GluRε4$^{-/-}$ mice ($p$ = 0.0001, paired $t$-test) in Session 1 compared with Session 8.

Mixed-design ANOVA of locomotor activity data during the 60 min period after the PCP injection revealed a significant effect of genotype ($F_{2,455}$ = 11.318, $p$<0.0001) but not session ($F_{7,455}$ = 1.443, $p$ = 0.186) and a significant genotype × session interaction ($F_{14,455}$ = 2.368, $p$ = 0.0035) (Fig. 5B). Phencyclidine-induced hyperactivity was significantly greater in Session 8 than Session 1 in wildtype mice ($p$ = 0.006, paired $t$-test). Repeated PCP (3 mg/kg) administration did not increase locomotor activity in GluRε1$^{-/-}$ mice ($p$ = 0.121, paired $t$-test) and GluRε4$^{-/-}$ mice ($p$ = 0.605, paired $t$-test) in Session 1 compared with Session 8.

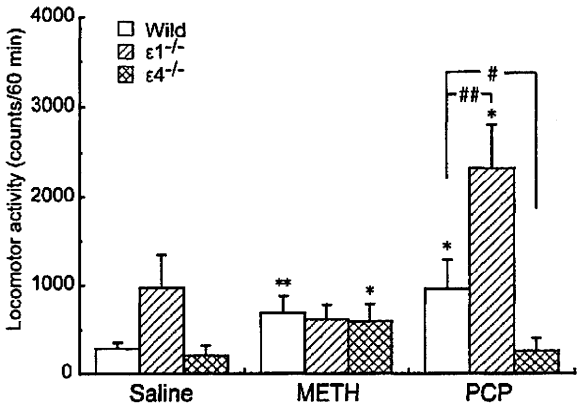


**Figure 4. Effects of acute METH and PCP on the locomotor activity in GluRε1$^{-/-}$ and GluRε4$^{-/-}$ mice.** Locomotor activity after acute saline, METH (1 mg/kg), or PCP (3 mg/kg) administration ($n = 10$–25). *$p<0.05$, **$p<0.01$, compared with saline (Student's $t$-test); #$p<0.05$, ##$p<0.01$, compared with wildtype (Student's $t$-test).
doi:10.1371/journal.pone.0013722.g004

## Discussion

The present study showed that PCP-induced increases in $DA_{ex}$ in the striatum and PFC and locomotor activity were absent in GluRε4$^{-/-}$, but present in GluRε1$^{-/-}$, mice, indicating that GluRε4 plays an important role in PCP-increased $DA_{ex}$ and locomotor activity. Phencyclidine exerts psychotomimetic effects, whereas another NMDA receptor antagonist, MK-801, exerts no clear psychotomimetic effects in humans [43]. Interestingly, whereas MK-801 suppresses GluRε3/GluRζ1 and GluRε4/GluRζ1 channels more weakly than GluRε1/GluRζ1 and GluRε2/GluRζ1 channels, PCP blocks the four GluRε/GluRζ channels to similar extents in *Xenopus* oocytes [32]. The absence of psychotomimetic effects of MK-801 may be attributable to its weak ability of blocking the GluRε4/GluRζ1 channel.

Systemic administration of PCP reportedly increases $DA_{ex}$ in the striatum and PFC [44–49]. Similarly, PCP (3 mg/kg) increased $DA_{ex}$ in wildtype and GluRε1$^{-/-}$ mice in the present study. However, PCP failed to increase $DA_{ex}$ in the striatum and PFC in GluRε4$^{-/-}$ mice. Phencyclidine is known to be a DA reuptake blocker and a noncompetitive NMDA antagonist [9–11]. It inhibits DA uptake by binding to the DAT at doses approximately 10-fold greater than those at which it binds to NMDA receptor channels [1]. Phencyclidine at the low dose used in the present study appears to have few effects on the DAT. Furthermore, no PCP-induced increases in $DA_{ex}$ in GluRε4$^{-/-}$ mice that possess an intact DAT gene indicates that PCP increases $DA_{ex}$ not via DAT inhibition but via blockade of NMDA receptor channels. The present results support the hypothesis that GluRε4 is an important determinant of increased $DA_{ex}$ induced by PCP. Acute administration of METH increased $DA_{ex}$ in the striatum and PFC in wildtype, GluRε1$^{-/-}$, and GluRε4$^{-/-}$ mice. No differences in $DA_{ex}$ increases were found between genotypes. The similar $DA_{ex}$ increases among these mice in response to acute METH challenge suggest that increased $DA_{ex}$ occurs independently of GluRε1$^{-/-}$ and GluRε4$^{-/-}$.

Locomotor activity in a novel environment is reportedly high in GluRε1$^{-/-}$ mice [34,36] and low in GluRε4$^{-/-}$ mice [33,35]. Consistent with these findings, increased locomotor activity in GluRε1$^{-/-}$ mice and reduced locomotor activity in GluRε4$^{-/-}$ mice were observed in the present study. GluRε1$^{-/-}$ mice did not habituate during the 180 min period compared with wildtype mice. Interestingly, acute METH administration decreased locomotor activity in GluRε1$^{-/-}$ mice. Hyperactivity and a paradoxical response to METH suggest that GluRε1$^{-/-}$ mice may be an animal model of attention-deficit/hyperactivity disorder.

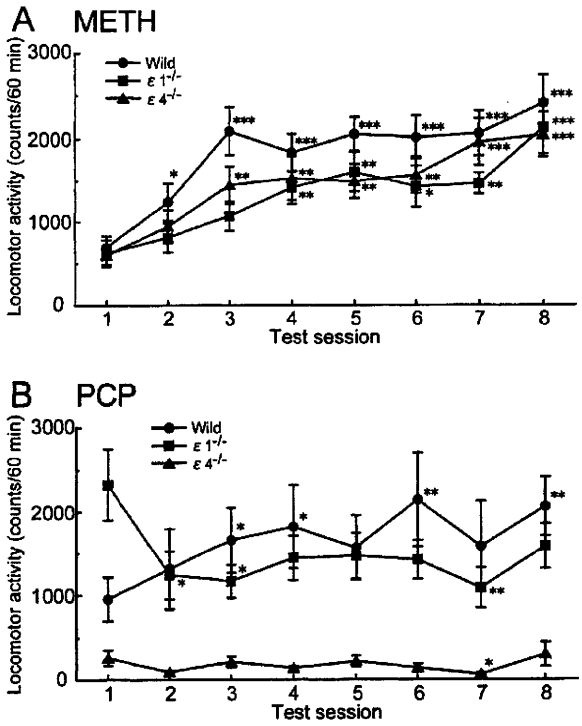


**Figure 5. Effects of repeated METH and PCP on the locomotor activity in GluRε1$^{-/-}$ and GluRε4$^{-/-}$ mice.** Changes in response to repeated administration of (**A**) METH (1 mg/kg) or (**B**) PCP (3 mg/kg) ($n = 15$–25). *$p<0.05$, **$p<0.01$, ***$p<0.001$, compared with Session 1 of the same genotype (paired $t$-test). Each point represents total locomotor activity (mean ± SEM) during the 60 min period after METH or PCP injection.
doi:10.1371/journal.pone.0013722.g005

Psychostimulants, such as METH and PCP, increase locomotor activity [2,3,12,13]. In GluRε4$^{-/-}$ mice, acute METH administration increased locomotor activity, but PCP did not. Acute PCP administration increased locomotor activity in wildtype and GluRε1$^{-/-}$ mice, but not in GluRε4$^{-/-}$ mice. The absence of locomotor-stimulating effects of PCP in GluRε4$^{-/-}$ mice indicates that locomotor responses to PCP require the GluRε4 subunit.

Repeated administration of PCP produces sensitization to its locomotor-stimulating effects in wildtype mice. In GluRε4$^{-/-}$ mice, locomotor activity did not increase after repeated PCP treatment. Acute PCP did not increase locomotor activity, and repeated PCP did not produce sensitization to the locomotor-stimulating effects of PCP in GluRε4$^{-/-}$ mice. The GluRε4 subunit appears to be necessary for behavioral sensitization to occur in response to repeated PCP administration. A previous study demonstrated that acute PCP treatment increased locomotor activity in wildtype and GluRε1$^{-/-}$ mice. Chronic PCP treatment at a low dose (3 mg/kg/day) for 7 days produced sensitization to the locomotor-stimulating effects of PCP in wildtype mice, but not

in GluRε1$^{-/-}$ mice [50]. The present study confirmed that repeated PCP administration (3 mg/kg/day) did not produce sensitization during Session 8 in GluRε1$^{-/-}$ mice. Repeated METH administration produced behavioral sensitization in wildtype, GluRε1$^{-/-}$, and GluRε4$^{-/-}$ mice. The development of sensitization in GluRε1$^{-/-}$ and GluRε4$^{-/-}$ mice was delayed compared with wildtype mice. The noncompetitive NMDA receptor antagonist MK-801 has been shown to block the development of behavioral sensitization to AMPH and METH [51–54]. Molecular and cellular adaptive changes during chronic drug exposure are hypothesized to lead to the development of sensitization. Our findings support the hypothesis that adaptive changes through NMDA receptor channels play a role in the development of locomotor sensitization to METH.

Schizophrenia is a disease that has been hypothesized to be associated with hyperfunction of the dopaminergic neuronal system and dysfunction of glutamatergic transmission [55,56]. Administration of PCP to normal humans induces symptoms similar to those of schizophrenia [57]. This finding has been replicated over the years, and PCP has been shown to exacerbate the primary symptoms of schizophrenic patients [56]. Phencyclidine-treated animals have been used as an animal model of schizophrenia, and the amelioration of hyperlocomotion in these animals has been used as a screening test to assess the efficacy of antipsychotic drugs [58,59]. GluRε4 immunoreactivity and protein expression increase in the frontal cortex following repeated PCP treatment, whereas GluRε1 immunoreactivity and protein expression are not altered in rats [60]. Furthermore, polymorphisms of several genes known to interact with NMDA receptor channels are related to altered risk for schizophrenia, and psychotic patients display changes in the levels of mRNA encoding NMDA receptors [61]. Interestingly, Makino *et al.* reported that the GluRε4 gene locus is a possible genomic region that contributes to schizophrenia susceptibility in a Japanese population [62]. In the present study, we first demonstrated that deletion of GluRε4 abolished PCP-induced hyperlocomotion and potentiated the increases in $DA_{ex}$ in mice. Our data and previous findings suggest that GluRε4 might be a potential target for antipsychotic drug development.

Although NMDA receptor channels are highly expressed in adult brains, adult GluRε4 expression is very limited [26]. GluRε4 is expressed in the substantia nigra compacta (SNc), subthalamic nucleus, globus pallidus, and ventral pallidum in adult rats [63]. Jones and Gibb reported that functional GluRε2 and GluRε4 subunits form somatic NMDA receptors, possibly as triheteromeric receptors, whereas no somatic GluRε1 subunits are present in SNc dopaminergic neurons in rats aged postnatal day 14 [64]. A small subset of NMDA receptor channels (i.e., channels containing GluRε4) may be implicated in the effects of PCP on $DA_{ex}$ and locomotor activity. This possibility is consistent with the lack of psychotic effects of ifenprodil, a selective blocker of NMDA receptor channels containing GluRε2, which is highly expressed in adult brains. Additionally, GluRε4 is highly expressed in the brain during development [26], suggesting that GluRε4 knockout during the developmental stage may alter neuronal function in the adult brain. Although the expression of the genes related to dopaminergic signaling pathways are not altered in GluRε4$^{-/-}$ mice during adulthood (see Table S1), other developmental changes may alter the effects of PCP in GluRε4$^{-/-}$ mice. Further studies of synapses, neurons, and neuronal networks regulated by GluRε4 and developmental changes in neuronal function in GluRε4$^{-/-}$ mice may lead to a better understanding of the mechanisms underlying PCP-induced psychosis and schizophrenia.

## Materials and Methods

### Ethics statement

The experimental procedures and housing conditions were approved by the Institutional Animal Care and Use Committee (Animal Experimentation Ethics Committee of Tokyo Institute of Psychiatry, Approval ID: 22-2), and all animal were cared for and treated humanely in accordance with our institutional animal experimentation guidelines.

### Animals

Wildtype and GluRε1$^{-/-}$ or GluRε4$^{-/-}$ mouse littermates from crosses of heterozygous/heterozygous GluRε1 or GluRε4 knockout mice, respectively, on a C57BL/6 genetic background [33,65] served as subjects. Naive adult mice were housed in an animal facility maintained at 22±2°C and 55±5% relative humidity under a 12 h/12 h light/dark cycle with lights on at 8:00 am and off at 8:00 pm. Food and water were available *ad libitum*. In the behavioral experiments, 13- to 23-week-old male mice were used. In the microdialysis experiments, 10- to 24-week-old male and female mice were used.

### Surgery

Microdialysis probes were stereotaxically implanted in mice under sodium pentobarbital anesthesia (50 mg/kg, intraperitoneally) in the striatum (anterior, +0.6 mm; lateral, +1.8 mm; ventral, −4.0 mm from bregma) or PFC (anterior, +2.0 mm; lateral, +0.5 mm; ventral −3.0 mm from bregma), according to the atlas of Franklin and Paxinos [66]. The probe tip was constructed with a regenerated cellulose membrane (outer diameter, 0.22 mm; membrane length, 2 mm; Eicom, Kyoto, Japan). All dialysis probe placements were verified histologically at the completion of the experiment.

### Microdialysis and analytical procedures

Twenty-four hours after implantation, the dialysis experiments were performed in freely moving animals. Ringer's solution (145 mM NaCl, 3 mM KCl, 1.26 mM $CaCl_2$, and 1 mM $MgCl_2$, pH 6.5) was perfused at a constant flow rate of 1 µl/min. Perfusates were directly injected into the high-performance liquid chromatography system every 10 min using an autoinjector (EAS-20; Eicom). Dialysate DA was separated using a reverse-phase ODS column (PP-ODS; Eicom) and detected with a graphite electrode (HTEC-500; Eicom). The mobile phase consisted of 0.1 M phosphate buffer (pH 5.5) containing 500 mg/l sodium decanesulfonate, 50 mg/l EDTA, and 1% methanol. Perfusion was initiated 180 min prior to the collection of baseline samples. Baseline levels of $DA_{ex}$ were obtained from the average concentrations of three consecutive samples when they were stable. The DA detection limit of the assay was 0.3 fmol/sample with a signal-to-noise ratio of 2.

### Locomotor activity measurements

Each mouse were exposed to an illuminated chamber (30×40×25 cm) at an ambient temperature of 22±2°C, and locomotor activity was measured with Supermex (Muromachi Kikai, Tokyo, Japan), a sensor monitor mounted above the chamber. In this system, a sensor detects the radiated body heat of an animal [67]. This measurement system can detect changes in heat across multiple zones of the chamber and count all horizontal movements. All counts were automatically summed and recorded every 5 min. After a 180 min habituation period, METH or PCP was administered subcutaneously (s.c.), and locomotor activity was monitored continuously for 180 min.

### Drugs

Drugs were dissolved in saline and administered s.c. in a volume of 10 ml/kg. In the microdialysis experiment, saline, METH (1 mg/kg), or PCP (3 mg/kg) was administered after establishing a stable baseline, and the dialysate was continuously collected for 180 min. In the acute behavioral experiments, saline, freshly prepared METH (1 mg/kg; Dainippon Sumitomo Pharma, Osaka, Japan), or PCP (3 mg/kg; Shionogi Pharmaceutical Co. Ltd., Osaka, Japan) was administered. In the repeated behavioral experiments, METH (1 mg/kg) or PCP (3 mg/kg) was administered repeatedly at 2 or 3 day intervals for a total of seven injections. One week after withdrawal, METH or PCP challenge injections were administered as described above.

### Statistical analysis

$DA_{ex}$ responses to drugs are expressed as a percentage of baseline. The AUC of $DA_{ex}$ during the 180 min period after drug administration was calculated as the effects of the drugs. Area-under-the-curve values of all groups were analyzed using two-way ANOVA. Individual *post hoc* comparisons were performed with Fisher's PLSD test. The responses to acute administration were analyzed using Student's *t*-test, one-way ANOVA, or two-way ANOVA. To evaluate behavioral sensitization, the response to drugs in Session 8 was compared with the response to the first drug injection (Session 1) in the same animal using a paired *t*-test or mixed-design ANOVA. Values of $p<0.05$ were considered statistically significant. Data were analyzed using Statview J5.0 software (SAS Institute, Cary, NC, USA).

## Supporting Information

**Table S1** Striatal gene expression in wildtype and GluRε4-/- mice.

Found at: doi:10.1371/journal.pone.0013722.s001 (0.03 MB DOC)

## Acknowledgments

We acknowledge Mr. Michael Arends for his assistance with editing the manuscript.

## Author Contributions

Conceived and designed the experiments: YH KI. Performed the experiments: YH HY. Analyzed the data: YH HY. Contributed reagents/materials/analysis tools: SK HY TN MM. Wrote the paper: YH WH TN MM KI.

## References


1. Javitt DC, Zukin SR (1991) Recent advances in the phencyclidine model of schizophrenia. Am J Psychiatry 148: 1301–1308.
2. Sturgeon RD, Fessler RG, Meltzer HY (1979) Behavioral rating scales for assessing phencyclidine-induced locomotor activity, stereotyped behavior and ataxia in rats. Eur J Pharmacol 59: 169–179.
3. Castellani S, Adams PM (1981) Acute and chronic phencyclidine effects on locomotor activity, stereotypy and ataxia in rats. Eur J Pharmacol 73: 143–154.
4. Nabeshima T, Fukaya H, Yamaguchi K, Ishikawa K, Furukawa H, et al. (1987) Development of tolerance and supersensitivity to phencyclidine in rats after repeated administration of phencyclidine. Eur J Pharmacol 135: 23–33.
5. Xu X, Domino EF (1994) Phencyclidine-induced behavioral sensitization. Pharmacol Biochem Behav 47: 603–608.
6. Anis NA, Berry SC, Burton NR, Lodge D (1983) The dissociative anaesthetics, ketamine and phencyclidine, selectively reduce excitation of central mammalian neurones by N-methyl-aspartate. Br J Pharmacol 79: 565–575.
7. Lodge D, Johnson KM (1990) Noncompetitive excitatory amino acid receptor antagonists. Trends Pharmacol Sci 11: 81–86.
8. Kemp JA, Foster AC, Wong EHF (1987) Non-competitive antagonists of excitatory amino acid receptors. Trends Neurosci 10: 294–298.
9. Smith RC, Meltzer HY, Arora RC, Davis JM (1977) Effects of phencyclidine on [3H]catecholamine and [3H]serotonin uptake in synaptosomal preparations from rat brain. Biochem Pharmacol 26: 1435–1439.
10. Snell LD, Yi SJ, Johnson KM (1988) Comparison of the effects of MK-801 and phencyclidine on catecholamine uptake and NMDA-induced norepinephrine release. Eur J Pharmacol 145: 223–226.
11. Garey RE, Heath RG (1976) The effects of phencyclidine on the uptake of $^3$H-catecholamines by rat striatal and hypothalamic synaptosomes. Life Sci 18: 1105–1110.
12. Pierce RC, Kalivas PW (1997) A circuitry model of the expression of behavioral sensitization to amphetamine-like psychostimulants. Brain Res Brain Res Rev 25: 192–216.
13. Robinson TE, Becker JB (1986) Enduring changes in brain and behavior produced by chronic amphetamine administration: a review and evaluation of animal models of amphetamine psychosis. Brain Res 396: 157–198.
14. Seiden LS, Sabol KE, Ricaurte GA (1993) Amphetamine: effects on catecholamine systems and behavior. Annu Rev Pharmacol Toxicol 33: 639–677.
15. Fischer JF, Cho AK (1979) Chemical release of dopamine from striatal homogenates: evidence for an exchange diffusion model. J Pharmacol Exp Ther 208: 203–209.
16. Schmitz Y, Lee CJ, Schmauss C, Gonon F, Sulzer D (2001) Amphetamine distorts stimulation-dependent dopamine overflow: effects on D2 autoreceptors, transporters, and synaptic vesicle stores. J Neurosci 21: 5916–5924.
17. Sulzer D, Maidment NT, Rayport S (1993) Amphetamine and other weak bases act to promote reverse transport of dopamine in ventral midbrain neurons. J Neurochem 60: 527–535.
18. Benwell ME, Balfour DJ, Lucchi HM (1993) Influence of tetrodotoxin and calcium on changes in extracellular dopamine levels evoked by systemic nicotine. Psychopharmacology (Berl) 112: 467–474.
19. Parker EM, Cubeddu LX (1988) Comparative effects of amphetamine, phenylethylamine and related drugs on dopamine efflux, dopamine uptake and mazindol binding. J Pharmacol Exp Ther 245: 199–210.
20. Heikkila RE, Orlansky H, Cohen G (1975) Studies on the distinction between uptake inhibition and release of [$^3$H]dopamine in rat brain tissue slices. Biochem Pharmacol 24: 847–852.
21. Horn AS, Coyle JT, Snyder SH (1971) Catecholamine uptake by synaptosomes from rat brain: structure-activity relationships of drugs with differential effects on dopamine and norepinephrine neurons. Mol Pharmacol 7: 66–80.
22. Green AL (1971) Inhibition of rat and mouse brain monoamine oxidases by (+)-amphetamine. Biochem J 121: 37P–38.
23. Green AL, el Hait MA (1978) Inhibition of mouse brain monoamine oxidase by (+)-amphetamine in vivo. J Pharm Pharmacol 30: 262–263.
24. Miller HH, Shore PA, Clarke DE (1980) In vivo monoamine oxidase inhibition by d-amphetamine. Biochem Pharmacol 29: 1347–1354.
25. Kew JN, Kemp JA (2005) Ionotropic and metabotropic glutamate receptor structure and pharmacology. Psychopharmacology (Berl) 179: 4–29.
26. Watanabe M, Inoue Y, Sakimura K, Mishina M (1992) Developmental changes in distribution of NMDA receptor channel subunit mRNAs. Neuroreport 3: 1138–1140.
27. Ikeda K, Nagasawa M, Mori H, Araki K, Sakimura K, et al. (1992) Cloning and expression of the ε4 subunit of the NMDA receptor channel. FEBS Lett 313: 34–38.
28. Kutsuwada T, Kashiwabuchi N, Mori H, Sakimura K, Kushiya E, et al. (1992) Molecular diversity of the NMDA receptor channel. Nature 358: 36–41.
29. Meguro H, Mori H, Araki K, Kushiya E, Kutsuwada T, et al. (1992) Functional characterization of a heteromeric NMDA receptor channel expressed from cloned cDNAs. Nature 357: 70–74.
30. Monyer H, Sprengel R, Schoepfer R, Herb A, Higuchi M, et al. (1992) Heteromeric NMDA receptors: molecular and functional distinction of subtypes. Science 256: 1217–1221.
31. Mori H, Mishina M (2003) Roles of diverse glutamate receptors in brain functions elucidated by subunit-specific and region-specific gene targeting. Life Sci 74: 329–336.
32. Yamakura T, Mori H, Masaki H, Shimoji K, Mishina M (1993) Different sensitivities of NMDA receptor channel subtypes to non-competitive antagonists. Neuroreport 4: 687–690.
33. Ikeda K, Araki K, Takayama C, Inoue Y, Yagi T, et al. (1995) Reduced spontaneous activity of mice defective in the ε4 subunit of the NMDA receptor channel. Brain Res Mol Brain Res 33: 61–71.
34. Miyamoto Y, Yamada K, Noda Y, Mori H, Mishina M, et al. (2001) Hyperfunction of dopaminergic and serotonergic neuronal systems in mice lacking the NMDA receptor ε1 subunit. J Neurosci 21: 750–757.
35. Miyamoto Y, Yamada K, Noda Y, Mori H, Mishina M, et al. (2002) Lower sensitivity to stress and altered monoaminergic neuronal function in mice lacking the NMDA receptor ε4 subunit. J Neurosci 22: 2335–2342.
36. Boyce-Rustay JM, Holmes A (2006) Genetic inactivation of the NMDA receptor NR2A subunit has anxiolytic- and antidepressant-like effects in mice. Neuropsychopharmacology 31: 2405–2414.

37. Kadotani H, Hirano T, Masugi M, Nakamura K, Nakao K, et al. (1996) Motor discoordination results from combined gene disruption of the NMDA receptor NR2A and NR2C subunits, but not from single disruption of the NR2A or NR2C subunit. J Neurosci 16: 7859–7867.
38. Ebralidze AK, Rossi DJ, Tonegawa S, Slater NT (1996) Modification of NMDA receptor channels and synaptic transmission by targeted disruption of the NR2C gene. J Neurosci 16: 5014–5025.
39. Sprengel R, Suchanek B, Amico C, Brusa R, Burnashev N, et al. (1998) Importance of the intracellular domain of NR2 subunits for NMDA receptor function in vivo. Cell 92: 279–289.
40. Kutsuwada T, Sakimura K, Manabe T, Takayama C, Katakura N, et al. (1996) Impairment of suckling response, trigeminal neuronal pattern formation, and hippocampal LTD in NMDA receptor ε2 subunit mutant mice. Neuron 16: 333–344.
41. Li Y, Erzurumlu RS, Chen C, Jhaveri S, Tonegawa S (1994) Whisker-related neuronal patterns fail to develop in the trigeminal brainstem nuclei of NMDAR1 knockout mice. Cell 76: 427–437.
42. Forrest D, Yuzaki M, Soares HD, Ng L, Luk DC, et al. (1994) Targeted disruption of NMDA receptor 1 gene abolishes NMDA response and results in neonatal death. Neuron 13: 325–338.
43. Troupin AS, Mendius, JR, Cheng, F, Risinger, MW (1986) MK-801. In: Meldrum BS, Porter RJ, eds. New anticonvulsant drugs (series title: Current problems in epilepsy, vol 4). London: Libbey. pp 191–201.
44. Chapman CD, Gazzara RA, Howard SG (1990) Effects of phencyclidine on extracellular levels of dopamine, dihydroxyphenylacetic acid and homovanillic acid in conscious and anesthetized rats. Neuropharmacology 29: 319–325.
45. Lillrank SM, O'Connor WT, Saransaari P, Ungerstedt U (1994) In vivo effects of local and systemic phencyclidine on the extracellular levels of catecholamines and transmitter amino acids in the dorsolateral striatum of anaesthetized rats. Acta Physiol Scand 150: 109–115.
46. Nishijima K, Kashiwa A, Hashimoto A, Iwama H, Umino A, et al. (1996) Differential effects of phencyclidine and methamphetamine on dopamine metabolism in rat frontal cortex and striatum as revealed by in vivo dialysis. Synapse 22: 304–312.
47. Hondo H, Yonezawa Y, Nakahara T, Nakamura K, Hirano M, et al. (1994) Effect of phencyclidine on dopamine release in the rat prefrontal cortex; an in vivo microdialysis study. Brain Res 633: 337–342.
48. Hertel P, Mathe JM, Nomikos GG, Iurlo M, Mathe AA, et al. (1995) Effects of D-amphetamine and phencyclidine on behavior and extracellular concentrations of neurotensin and dopamine in the ventral striatum and the medial prefrontal cortex of the rat. Behav Brain Res 72: 103–114.
49. Adams B, Moghaddam B (1998) Corticolimbic dopamine neurotransmission is temporally dissociated from the cognitive and locomotor effects of phencyclidine. J Neurosci 18: 5545–5554.
50. Miyamoto Y, Yamada K, Nagai T, Mori H, Mishina M, et al. (2004) Behavioural adaptations to addictive drugs in mice lacking the NMDA receptor $\varepsilon_1$ subunit. Eur J Neurosci 19: 151–158.
51. Ohmori T, Abekawa T, Muraki A, Koyama T (1994) Competitive and noncompetitive NMDA antagonists block sensitization to methamphetamine. Pharmacol Biochem Behav 48: 587–591.
52. Wolf ME, Khansa MR (1991) Repeated administration of MK-801 produces sensitization to its own locomotor stimulant effects but blocks sensitization to amphetamine. Brain Res 562: 164–168.
53. Wolf ME, Jeziorski M (1993) Coadministration of MK-801 with amphetamine, cocaine or morphine prevents rather than transiently masks the development of behavioral sensitization. Brain Res 613: 291–294.
54. Kuribara H, Asami T, Ida I, Iijima Y, Tadokoro S (1992) Effects of repeated MK-801 on ambulation in mice and in sensitization following methamphetamine. Psychopharmacology (Berl) 108: 271–275.
55. Carlsson A, Waters N, Waters S, Carlsson ML (2000) Network interactions in schizophrenia: therapeutic implications. Brain Res Brain Res Rev 31: 342–349.
56. Jentsch JD, Roth RH (1999) The neuropsychopharmacology of phencyclidine: from NMDA receptor hypofunction to the dopamine hypothesis of schizophrenia. Neuropsychopharmacology 20: 201–225.
57. Luby ED, Cohen BD, Rosenbaum G, Gottlieb JS, Kelley R (1959) Study of a new schizophrenomimetic drug; sernyl. AMA Arch Neurol Psychiatry 81: 363–369.
58. Mouri A, Noda Y, Enomoto T, Nabeshima T (2007) Phencyclidine animal models of schizophrenia: approaches from abnormality of glutamatergic neurotransmission and neurodevelopment. Neurochem Int 51: 173–184.
59. Geyer MA, Ellenbroek B (2003) Animal behavior models of the mechanisms underlying antipsychotic atypicality. Prog Neuropsychopharmacol Biol Psychiatry 27: 1071–1079.
60. Lindahl JS, Keifer J (2004) Glutamate receptor subunits are altered in forebrain and cerebellum in rats chronically exposed to the NMDA receptor antagonist phencyclidine. Neuropsychopharmacology 29: 2065–2073.
61. Millan MJ (2005) *N*-methyl-D-aspartate receptors as a target for improved antipsychotic agents: novel insights and clinical perspectives. Psychopharmacology (Berl) 179: 30–53.
62. Makino C, Shibata H, Ninomiya H, Tashiro N, Fukumaki Y (2005) Identification of single-nucleotide polymorphisms in the human *N*-methyl-D-aspartate receptor subunit NR2D gene, *GRIN2D*, and association study with schizophrenia. Psychiatr Genet 15: 215–221.
63. Standaert DG, Testa CM, Young AB, Penney JB, Jr. (1994) Organization of N-methyl-D-aspartate glutamate receptor gene expression in the basal ganglia of the rat. J Comp Neurol 343: 1–16.
64. Jones S, Gibb AJ (2005) Functional NR2B- and NR2D-containing NMDA receptor channels in rat substantia nigra dopaminergic neurones. J Physiol 569: 209–221.
65. Sakimura K, Kutsuwada T, Ito I, Manabe T, Takayama C, et al. (1995) Reduced hippocampal LTP and spatial learning in mice lacking NMDA receptor ε1 subunit. Nature 373: 151–155.
66. Franklin KBJ, Paxinos G (1997) The mouse brain in stereotaxic coordinates. San Diego: Academic Press.
67. Masuo Y, Matsumoto Y, Morita S, Noguchi J (1997) A novel method for counting spontaneous motor activity in the rat. Brain Res Brain Res Protoc 1: 321–326.

**Neuropsychopharmacology (2010) 35,** 1560–1569

**www.neuropsychopharmacology.org**

# Inhibition of G-Protein-Activated Inwardly Rectifying $K^+$ Channels by the Selective Norepinephrine Reuptake Inhibitors Atomoxetine and Reboxetine

**Toru Kobayashi*[,1], Kazuo Washiyama[1] and Kazutaka Ikeda[2]**

*[1]Department of Molecular Neuropathology, Brain Research Institute, Niigata University, Chuo-ku, Niigata, Niigata, Japan; [2]Division of Psychobiology, Tokyo Institute of Psychiatry, Setagaya-ku, Tokyo, Japan*

Atomoxetine and reboxetine are commonly used as selective norepinephrine reuptake inhibitors (NRIs) for the treatment of attention-deficit/hyperactivity disorder and depression, respectively. Furthermore, recent studies have suggested that NRIs may be useful for the treatment of several other psychiatric disorders. However, the molecular mechanisms underlying the various effects of NRIs have not yet been sufficiently clarified. G-protein-activated inwardly rectifying $K^+$ (GIRK or Kir3) channels have an important function in regulating neuronal excitability and heart rate, and GIRK channel modulation has been suggested to be a potential treatment for several neuropsychiatric disorders and cardiac arrhythmias. In this study, we investigated the effects of atomoxetine and reboxetine on GIRK channels using the *Xenopus* oocyte expression assay. In oocytes injected with mRNA for GIRK1/GIRK2, GIRK2, or GIRK1/GIRK4 subunits, extracellular application of atomoxetine or reboxetine reversibly reduced GIRK currents. The inhibitory effects were concentration-dependent, but voltage-independent, and time-independent during each voltage pulse. However, Kir1.1 and Kir2.1 channels were insensitive to atomoxetine and reboxetine. Atomoxetine and reboxetine also inhibited GIRK currents induced by activation of cloned $A_1$ adenosine receptors or by intracellularly applied GTPγS, a nonhydrolyzable GTP analogue. Furthermore, the GIRK currents induced by ethanol were concentration-dependently inhibited by extracellularly applied atomoxetine but not by intracellularly applied atomoxetine. The present results suggest that atomoxetine and reboxetine inhibit brain- and cardiac-type GIRK channels, revealing a novel characteristic of clinically used NRIs. GIRK channel inhibition may contribute to some of the therapeutic effects of NRIs and adverse side effects related to nervous system and heart function.
*Neuropsychopharmacology* (2010) **35,** 1560–1569; doi:10.1038/npp.2010.27; published online 10 March 2010

**Keywords:** atomoxetine; reboxetine; selective norepinephrine reuptake inhibitor; GIRK channel; ethanol; *Xenopus* oocyte

## INTRODUCTION

Atomoxetine (originally named tomoxetine) and reboxetine are commonly used as selective norepinephrine reuptake inhibitors (NRIs) for the treatment of attention-deficit/hyperactivity disorder and depression, respectively (Hajós *et al*, 2004; Garland and Kirkpatrick 2004; Simpson and Plosker, 2004; Supplementary Figure S1). Their clinical efficacy is hypothesized to be linked mainly with potent inhibition of presynaptic norepinephrine transporters (Wong *et al*, 2000; Hajós *et al*, 2004; Simpson and Plosker, 2004). Furthermore, recent studies have suggested that the drugs are potentially useful for the treatment of several other psychiatric conditions, including anxiety disorders, eating disorders, substance use disorders, and narcolepsy (Kadhe *et al*, 2003; Hajós *et al*, 2004; Szerman *et al*, 2005; McElroy *et al*, 2007; Geller *et al*, 2007; Wilens *et al*, 2008). However, the molecular mechanisms underlying the various effects of NRIs have not yet been sufficiently clarified.

G-protein-activated inwardly rectifying $K^+$ (GIRK) channels (also known as Kir3 channels) are members of a major subfamily of inwardly rectifying $K^+$ (Kir) channels that include seven subfamilies (Reimann and Ashcroft, 1999). Four GIRK channel subunits have been identified in mammals (Kubo *et al*, 1993b; Krapivinsky *et al*, 1995; Lesage *et al*, 1995). Neuronal GIRK channels are predominantly heteromultimers composed of GIRK1 and GIRK2 subunits in most brain regions or homomultimers composed of GIRK2 subunits in the substantia nigra (Lesage *et al*, 1995; Karschin *et al*, 1996; Liao *et al*, 1996; Inanobe *et al*, 1999), whereas atrial GIRK channels are heteromultimers composed of GIRK1 and GIRK4 subunits (Krapivinsky *et al*, 1995). The channels are activated by various

*Correspondence: Dr T Kobayashi, Department of Molecular Neuropathology, Brain Research Institute, Niigata University, 1-757 Asahimachi, Chuo-ku, Niigata, Niigata 951-8585, Japan, Tel: +81 25 227 0646, Fax: +81 25 227 0818, E-mail: torukoba@bri.niigata-u.ac.jp
Received 4 November 2009; revised 30 January 2010; accepted 8 February 2010

$G_i$-protein-coupled receptors, such as $M_2$ muscarinic, $\alpha_2$ adrenergic, $D_2$ dopaminergic, opioid, nociceptin/orphanin FQ, $CB_1$ cannabinoid, and $A_1$ adenosine receptors, through the direct action of G-protein $\beta\gamma$ subunits (North, 1989; Dascal, 1997; Kobayashi and Ikeda, 2006). Additionally, ethanol activates GIRK channels independently of G-protein-coupled signaling pathways (Kobayashi *et al*, 1999; Lewohl *et al*, 1999). GIRK channels have an important function in regulating neuronal excitability, synaptic transmission, and heart rate (North, 1989; Lüscher *et al*, 1997; Signorini *et al*, 1997; Kuzhikandathil and Oxford, 2002; Kovoor *et al*, 2001). Furthermore, recent studies have suggested that GIRK channel modulation has the potential for treating several neuropsychiatric disorders and cardiac arrhythmias (Hashimoto *et al*, 2006; Kobayashi and Ikeda 2006; Cruz *et al*, 2008). Therefore, GIRK channel modulators may affect various brain and cardiac functions. In this study, the effects of atomoxetine and reboxetine on GIRK channels were examined using the *Xenopus* oocyte expression assay.

## MATERIALS AND METHODS

### Preparation of Specific mRNAs

Plasmids containing the entire coding sequences for the mouse GIRK1, GIRK2, and GIRK4 channel subunits and the *Xenopus* $A_1$ adenosine receptor ($A_1R$) were obtained previously (Kobayashi *et al*, 1995, 1999, 2000, 2002). cDNAs for rat Kir1.1 in pSPORT (Ho *et al*, 1993) and mouse Kir2.1 in pcDNA1 (Kubo *et al*, 1993a) were generously provided by Dr Steven C Hebert (Yale University) and Dr Lily Y Jan (University of California, San Francisco), respectively. These plasmids were linearized by digestion with the appropriate enzymes as described previously (Ho *et al*, 1993; Kubo *et al*, 1993a; Kobayashi *et al*, 2000). The specific mRNAs were synthesized *in vitro* using the mMESSAGE mMACHINE *in vitro* transcription kit (Ambion, Austin, TX, USA).

### Electrophysiological Analysis

Adult female *Xenopus laevis* frogs (Copacetic, Soma, Aomori, Japan) were anesthetized by immersion in water containing 0.15% tricaine (Sigma-Aldrich, St Louis, MO, USA). A small incision was made on the abdomen to remove several ovarian lobes from the frogs, which were humanely killed after the final collection. All procedures for the care and treatment of animals were carried out in accordance with National Institutes of Health guidelines and were approved by our Institutional Animal Care and Use Committee. *Xenopus* oocytes (Stages V and VI) were manually isolated from the ovary and maintained in Barth's solution (Kobayashi *et al*, 2002). Oocytes were injected with mRNA for GIRK1/GIRK2 or GIRK1/GIRK4 combinations (each 0.15 ng), GIRK2 (1 ng), Kir1.1 (2 ng), Kir2.1 (0.3 ng), or $A_1R$ (5 ng). The oocytes were incubated at 19°C in Barth's solution and manually defolliculated after treatment with 0.8 mg $ml^{-1}$ collagenase (Wako Pure Chemical Industries, Osaka, Japan) for 1 h. Whole-cell currents of the oocytes were recorded 3–8 days after injection with a conventional two-electrode voltage clamp (Kobayashi *et al*, 1999; Ikeda *et al*, 2003). All recordings were carried out at room temperature (19°C) to avoid damage to *Xenopus* oocytes and the effects of temperature (Fraser and Djamgoz, 1992; Weber, 1999). The membrane potential was held at −70 mV unless otherwise specified. Microelectrodes were filled with 3 M KCl. The oocytes were placed in a 0.05 ml narrow chamber and continuously superfused with a high-potassium (hK) solution (96 mM KCl, 2 mM NaCl, 1 mM $MgCl_2$, 1.5 mM $CaCl_2$, and 5 mM HEPES, pH 7.4 with KOH) or a $K^+$-free high-sodium (ND98) solution (98 mM NaCl, 1 mM $MgCl_2$, 1.5 mM $CaCl_2$, and 5 mM HEPES, pH 7.4 with NaOH) at a flow rate of 2.5 ml/min. In the hK solution, the $K^+$ equilibrium potential was close to 0 mV, and the inward $K^+$ current flow through the Kir channels was observed at negative holding potentials as shown earlier (Ho *et al*, 1993; Kubo *et al*, 1993a; Lesage *et al*, 1995; Kobayashi *et al*, 2006). Additionally, to examine the effects of the NRIs on outward $K^+$ currents, a perfusion solution containing 4 mM $K^+$ (K4 solution) was made by substituting NaCl with KCl in the ND98 solution. To examine the effects of the drugs on GIRK channels activated by G-protein activation, 13.8 nl of 100 mM $Li_4$-guanosine-5′-O-(3-thiotriphosphate) (GTPγS; Sigma-Aldrich), a nonhydrolyzable G-protein activator, dissolved in distilled water was injected into an oocyte using a nanoliter injector (World Precision Instruments, Sarasota, FL, USA) as described earlier (Kovoor *et al*, 1995). Furthermore, to examine the effects of intracellular atomoxetine, 23 nl of 10 mM atomoxetine dissolved in distilled water was injected into an oocyte using a nanoliter injector (Kobayashi *et al*, 2003), and the oocyte currents were then continuously recorded for ~30–40 min. As the volume of the *Xenopus* oocytes used was ~1 μl, the intracellular concentration of atomoxetine was presumed to be ~225 μM. For analysis of concentration–response relationships, data were fitted to the following logistic equation: drug inhibition = max/1 + $(EC_{50}/[drug])^{nH}$, with max being the maximal inhibition attainable, $EC_{50}$ being the concentration of a drug that produces 50% of the maximal current response for that drug, [drug] being the concentration of an NRI and $n_H$ being the Hill coefficient, using KaleidaGraph (Synergy Software, Reading, PA, USA). The concentrations required to reduce control currents, by 25 and 50% ($IC_{25}$ and $IC_{50}$, respectively), were calculated from the concentration–response relationships.

### Statistical Analysis

Data are expressed as mean ± SEM, and $n$ is the number of oocytes tested. Statistical analysis of the differences between groups was performed using Student's $t$-test, paired $t$-test, one-way analysis of variance (ANOVA), or two-way ANOVA followed by Tukey–Kramer *post hoc* test. Values of $P<0.05$ were considered statistically significant.

### Compounds

Tomoxetine hydrochloride (recently renamed atomoxetine hydrochloride) and reboxetine mesylate were purchased from Tocris Cookson (Bristol, UK) and dissolved in dimethyl sulfoxide (DMSO) or distilled water. The stock solution of each compound was stored at −30°C until use. Ethanol was purchased from Wako Pure Chemical Industries.

Each compound was added to the perfusion solution in appropriate amounts immediately before the experiments.

## RESULTS

### Inhibition of GIRK Channels by Atomoxetine and Reboxetine

In *Xenopus* oocytes injected with GIRK1 and GIRK2 mRNAs, basal GIRK currents, which depend on free G-protein $\beta\gamma$ subunits present in the oocytes because of the inherent activity of G-proteins (Dascal, 1997), were observed at a holding potential of −70 mV in an hK solution containing 96 mM $K^+$ (Figure 1a). Extracellular application of 30 μM atomoxetine or reboxetine reversibly reduced the inward currents through the expressed GIRK channels (Figure 1a). The current responses to an additional 100 μM atomoxetine during the application of 3 mM $Ba^{2+}$, which blocks Kir channels, were not significant (reduction of inward currents by 5.5 ± 5.0 nA; <1% inhibition of the $Ba^{2+}$-sensitive current components; $n = 4$). The 3 mM $Ba^{2+}$-sensitive current components (910.5 ± 65.7 nA, $n = 14$) are considered to correspond to the magnitude of GIRK currents in oocytes expressing GIRK channels (Kobayashi *et al*, 1999). Atomoxetine and reboxetine produced no significant response in a $K^+$-free ND98 perfusion solution containing 98 mM $Na^+$ instead of the hK solution ($n = 4$; data not shown), suggesting that the NRI-sensitive current components show $K^+$ selectivity. Additionally, application of DMSO or distilled water, the solvent vehicle, at the highest concentration (0.3%) induced no significant current response in the hK or ND98 solutions ($n = 5$; data not shown). However, in oocytes injected with mRNA for Kir1.1, an ATP-regulated Kir channel (Ho *et al*, 1993), or Kir2.1, a constitutively active Kir channel (Kubo *et al*, 1993a), extracellular application of 300 μM atomoxetine or reboxetine had no significant effects on the inward currents through the channels in the hK solution (<3% change of the $Ba^{2+}$-sensitive current components; 583.3 ± 59.7 nA for Kir1.1, $n = 4$; 1306.7 ± 179.8 nA for Kir2.1, $n = 4$; Figure 1b). In uninjected oocytes, 300 μM atomoxetine and reboxetine as well as 3 mM $Ba^{2+}$ caused no significant response (3.8 ± 2.9, 0 ± 0, and 6.8 ± 0.7 nA, respectively; $n = 4$, 4, and 7, respectively; Figure 1c) compared with oocytes injected with GIRK mRNA, suggesting no significant effects of atomoxetine, reboxetine, or $Ba^{2+}$ on intrinsic oocyte channels. Furthermore, in oocytes injected with GIRK1 and GIRK2 mRNAs, outward currents observed at a holding potential of −30 mV in a K4 solution containing 4 mM $K^+$ were reversibly reduced by 30 μM atomoxetine ($n = 4$), 30 μM reboxetine ($n = 4$), or 3 mM $Ba^{2+}$ (the $Ba^{2+}$-sensitive current components, 85.2 ± 32.8 nA, $n = 8$; Supplementary Figure S2), whereas in uninjected oocytes, the NRIs at 100 μM and 3 mM $Ba^{2+}$ caused no significant response (3.0 ± 0.9 nA for atomoxetine, 0 ± 0 nA for reboxetine, and 7.6 ± 1.3 nA for $Ba^{2+}$; $n = 4$, 4, and 8, respectively). The results suggest that the NRIs also inhibited outward GIRK currents. Similarly, in oocytes injected with either GIRK1 and GIRK4 mRNAs or GIRK2 mRNA, atomoxetine and reboxetine inhibited basal GIRK currents under the same conditions (3 mM $Ba^{2+}$-sensitive current components for GIRK1/4, 1027.5 ± 112.6 nA, $n = 10$; 3 mM $Ba^{2+}$-sensitive current components for GIRK2, 757.0 ± 51.5 nA, $n = 12$; Figure 2). The results suggest that atomoxetine and reboxetine inhibited GIRK channels, but not Kir1.1 and Kir2.1 channels.

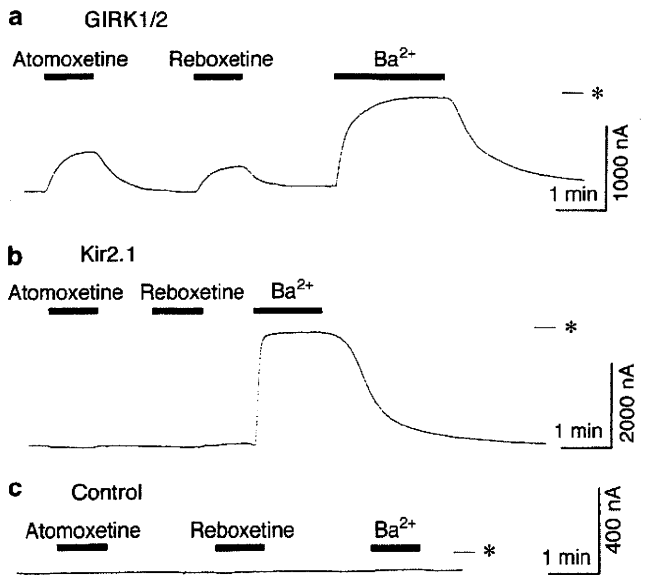


**Figure 1** Inhibitory effects of atomoxetine and reboxetine on GIRK channels expressed in *Xenopus* oocytes. (a) In an oocyte injected with GIRK1 and GIRK2 mRNAs, current responses to 10 μM atomoxetine, 10 μM reboxetine, and 3 mM $Ba^{2+}$ are shown. (b) In an oocyte injected with Kir2.1 mRNA, current responses to 100 μM atomoxetine, 100 μM reboxetine, and 3 mM $Ba^{2+}$ are shown. (c) In an uninjected oocyte, no significant current responses to 300 μM atomoxetine, 300 μM reboxetine, or 3 mM $Ba^{2+}$ are shown. Current responses were measured at a membrane potential of −70 mV in an hK solution containing 96 mM $K^+$. Asterisks show the zero current level. Horizontal bars indicate the duration of application.

### Characteristics of Inhibition of GIRK Channels by Atomoxetine and Reboxetine

The concentration–response relationships of the inhibitory effects of atomoxetine and reboxetine on GIRK1/2, GIRK2, and GIRK1/4 channels were investigated. Figure 2 shows that inhibition of these types of GIRK channels by atomoxetine and reboxetine was concentration-dependent. Table 1 shows the $EC_{50}$ and $n_H$ values obtained from the concentration–response relationships and the percentage inhibition of the GIRK currents by the NRIs at the highest concentrations tested. Additionally, because the drugs could not completely block these types of GIRK channels, even at the highest concentrations tested, the $IC_{25}$ and $IC_{50}$ values were also calculated to further compare the effects of the drugs (Table 1). The inhibition of GIRK1/4 channels by atomoxetine was more effective at 10 and 30 μM than inhibition of GIRK2 channels ($P < 0.05$, Tukey–Kramer *post hoc* test), although the effects of atomoxetine at the highest concentration on three types of channels were similar ($P > 0.05$, Tukey–Kramer *post hoc* test; Figure 2a; Table 1). In contrast, the inhibitory effects of reboxetine on these types of channels were statistically similar ($P > 0.05$ at each concentration, Tukey–Kramer *post hoc* test), although the inhibition of GIRK2 channels by 100 and 300 μM reboxetine was slightly less effective than inhibition of the other

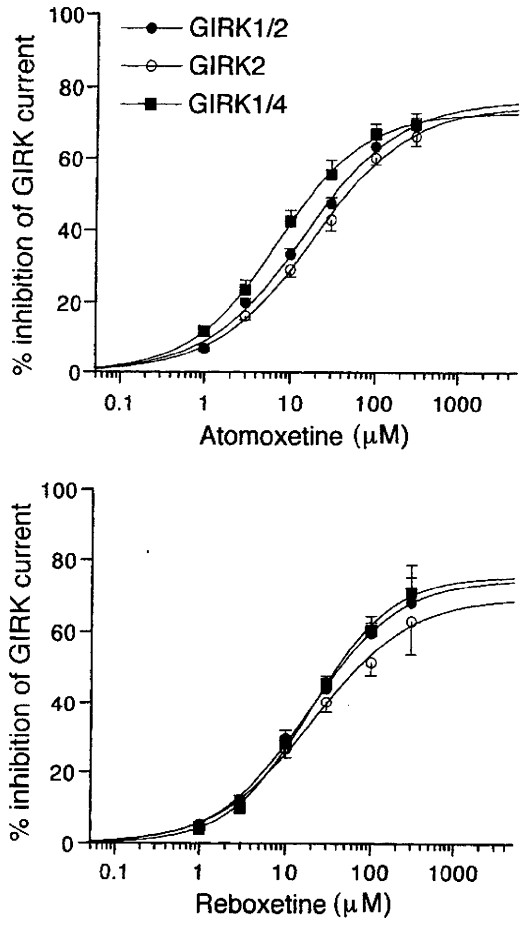


**Figure 2** Concentration–response relationships for the inhibitory effects of atomoxetine and reboxetine on GIRK1/2, GIRK2, and GIRK1/4 channels. The magnitudes of inhibition of GIRK currents by the drugs were compared with the 3 mM $Ba^{2+}$-sensitive current components in oocytes expressing GIRK1/2, GIRK2, and GIRK1/4 channels (910.5 ± 65.7 nA, $n = 14$; 757.0 ± 51.5 nA, $n = 12$; and 1027.5 ± 112.6 nA, $n = 10$, respectively). Each point and error bar represents the mean ± SEM of the percentage responses.

**Table 1** Inhibitory Effects of Atomoxetine and Reboxetine on GIRK Channels

| | Atomoxetine | | | Reboxetine | | |
|---|---|---|---|---|---|---|
| | **GIRK1/2** | **GIRK2** | **GIRK1/4** | **GIRK1/2** | **GIRK2** | **GIRK1/4** |
| $EC_{50}$ (μM) | 10.9 ± 1.3 | 12.4 ± 1.5 | 6.5 ± 0.4 | 13.7 ± 1.3 | 15.5 ± 2.1 | 19.4 ± 1.7 |
| $IC_{25}$ (μM) | 5.4 ± 0.4 | 6.1 ± 0.5 | 2.9 ± 0.2 | 7.8 ± 1.1 | 8.8 ± 1.4 | 9.0 ± 0.4 |
| $IC_{50}$ (μM) | 33.3 ± 4.9 | 52.2 ± 10.2 | 14.3 ± 1.6 | 48.2 ± 11.1 | 64.0 ± 18.3 | 41.0 ± 4.9 |
| % Max | 69.3 ± 2.5 | 67.0 ± 1.3 | 73.1 ± 0.8 | 68.3 ± 10.6 | 63.1 ± 9.1 | 71.1 ± 4.2 |
| ($n$) | (8) | (6) | (5) | (6) | (6) | (5) |
| $n_H$ | 0.96 ± 0.09 | 0.89 ± 0.09 | 0.88 ± 0.07 | 0.94 ± 0.03 | 0.91 ± 0.04 | 0.93 ± 0.04 |

Mean ± SEM of the concentration of a drug that produces 50% of the maximal effect ($EC_{50}$) and the concentrations required to reduce basal GIRK currents by 25 and 50% ($IC_{25}$ and $IC_{50}$, respectively) are shown in μM. The values of % max indicate the mean ± SEM percentage inhibition of basal GIRK currents by a drug at the highest concentrations tested (300 μM). The number of *Xenopus* oocytes tested ($n$) is indicated in parentheses. The $n_H$ values indicate the mean ± SEM of Hill coefficients.

channel types (Figure 2b). Furthermore, inhibition of GIRK1/4 channels by 10 μM atomoxetine was more effective than 10 μM reboxetine ($P < 0.05$, Tukey–Kramer *post hoc* test), whereas the effects of atomoxetine on GIRK1/2 and GIRK2 channels were similar to reboxetine ($P > 0.05$ at each concentration, Tukey–Kramer *post hoc* test).

Instantaneous GIRK1/2 currents elicited by the voltage step to −100 mV from a holding potential of 0 mV were diminished in the presence of 30 μM atomoxetine applied for 3 min (Figure 3a). The percentage inhibition of the steady-state GIRK current at the end of the voltage step by atomoxetine was not significantly different from that of the instantaneous current ($P > 0.05$, paired $t$-test; $n = 9$ at −40, −60, −80, −100, and −120 mV, respectively). For reboxetine, similar results were observed ($n = 7$). These results suggest that the channels were inhibited by atomoxetine and reboxetine primarily at the holding potential of 0 mV and time-independently during each voltage pulse. Similar to the 3 mM $Ba^{2+}$-sensitive current components corresponding to the magnitudes of basal GIRK currents, the magnitudes of currents reduced by 30 μM atomoxetine in oocytes expressing GIRK1/2 channels increased with negative membrane potentials, and the current–voltage relationships showed strong inward rectification ($n = 9$; Figure 3b), indicating a characteristic of GIRK currents. The percentage inhibition of GIRK1/2 currents by 30 μM atomoxetine showed no significant difference across voltages between −120 and −40 mV (no significant atomoxetine effect × membrane potential effect interaction, $P > 0.1$, one-way ANOVA; $P > 0.1$ across voltages, Tukey–Kramer *post hoc* test; Figure 3c). For reboxetine, similar results were observed ($n = 7$; Figure 3b and c). The results suggest that the inhibition of GIRK channels by atomoxetine and reboxetine was voltage-independent. Furthermore, similar results were obtained in oocytes expressing GIRK1/4 channels ($n = 5$ for atomoxetine and $n = 4$ for reboxetine; data not shown). Therefore, atomoxetine and reboxetine may have similar actions as GIRK channel inhibitors.

Atomoxetine possesses a secondary amine group with a $pK_a$ value of 9.23 (Eli Lilly and Company Data Sheet; Supplementary Figure S1). At physiological pH or below, atomoxetine exists mainly in a protonated form, ~98.5% at pH 7.4, and the proportion of the uncharged form increases with an increase in pH. We examined whether changes in extracellular pH would affect GIRK channel inhibition by atomoxetine. However, in oocytes expressing GIRK1/2 channels, the percentage inhibition of GIRK channels by atomoxetine at the same concentrations was not significantly affected by extracellular pH 7.4 and 9.2 (no significant pH × atomoxetine interaction, $P > 0.5$, two-way ANOVA; $P > 0.1$ at each concentration, Tukey–Kramer *post hoc* test; Figure 4). The results indicate that a marked increase in the proportion of the uncharged form may not significantly affect all of the effects on GIRK channels, suggesting that GIRK channel inhibition may be mediated by both forms of atomoxetine with similar effectiveness.

## Effects of Atomoxetine and Reboxetine on GIRK Channels Activated by a G-Protein-Coupled Receptor or GTPγS

We examined the effects of atomoxetine and reboxetine on GIRK channels activated by a G-protein-coupled receptor.

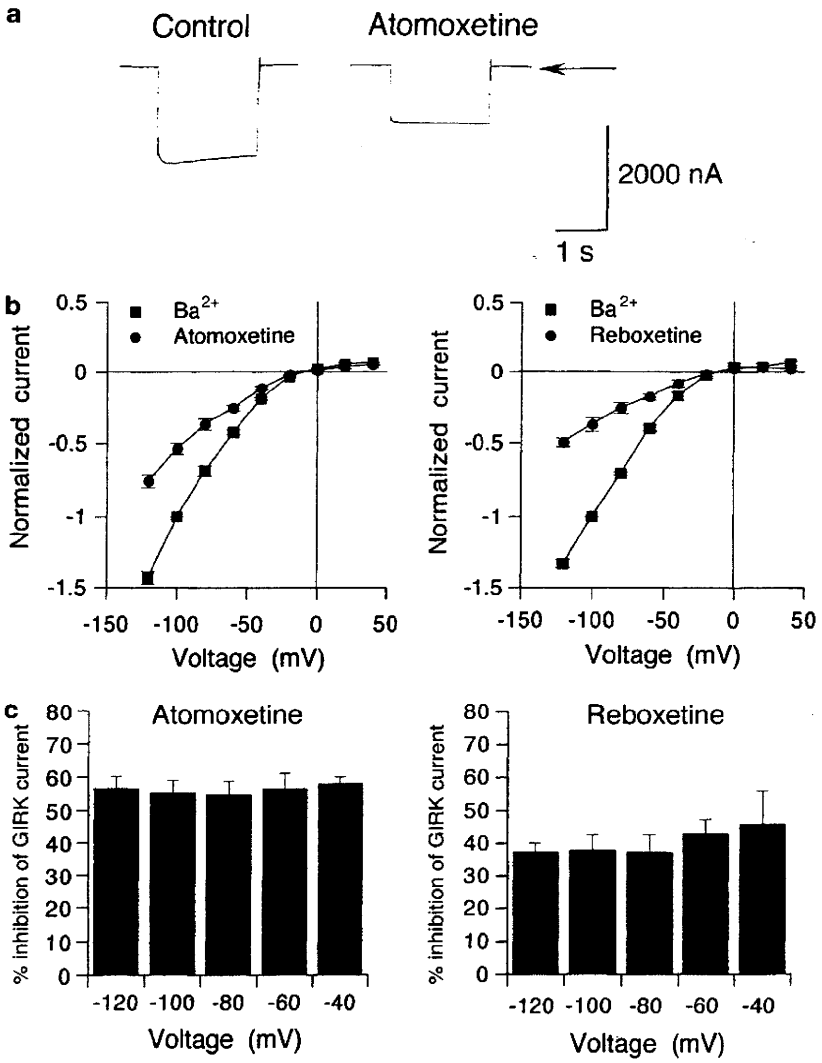


**Figure 3** Characteristics of the inhibitory effects of atomoxetine and reboxetine on GIRK currents. (a) Representative GIRK1/2 currents elicited by a voltage step to −100 mV for 2 s from a holding potential of 0 mV in the presence or absence of 30 μM atomoxetine applied for 3 min. Current responses were recorded in an hK solution containing 96 mM $K^+$. Arrow indicates the zero current level. (b) Current–voltage relationships of the magnitudes of the current component sensitive to 3 mM $Ba^{2+}$ and the magnitudes of currents reduced by 30 μM atomoxetine (left) or 30 μM reboxetine (right) in oocytes expressing GIRK1/2 channels. Current responses to a drug were normalized to the 3 mM $Ba^{2+}$-sensitive current component measured at a membrane potential of −100 mV (1219.7 ± 79.2 nA, $n = 14$). (c) Percentage inhibition of GIRK1/2 channels by atomoxetine or reboxetine over the voltage range of −120 to −40 mV. The magnitudes of inhibition of GIRK currents by 30 μM atomoxetine (left, $n = 8$) or 30 μM reboxetine (right, $n = 6$) at the end of the voltage pulses were compared with the 3 mM $Ba^{2+}$-sensitive current components. All values are expressed as mean ± SEM.

In oocytes co-expressing GIRK1/2 channels and $A_1$Rs (Kobayashi *et al*, 2002), 100 nM adenosine significantly induced inward GIRK currents (1000.7 ± 76.9 nA, $n = 10$; Figure 5a), and 300 μM atomoxetine or reboxetine alone consistently inhibited basal GIRK currents (3 mM $Ba^{2+}$-sensitive current components, 157.2 ± 31.3 nA, $n = 10$). The current responses to 100 nM adenosine were reduced by the addition of atomoxetine or reboxetine ($n = 5$ for each NRI; Figure 5a). These results suggest that atomoxetine and reboxetine inhibited total GIRK currents through the GIRK channels activated by the $A_1$R and the basally active GIRK channels. The percentage inhibition of total GIRK currents by atomoxetine or reboxetine ($IC_{25} = 4.5 \pm 1.6$ and 8.6 ± 1.7 μM; $IC_{50} = 42.7 \pm 12.3$ and 55.1 ± 16.4 μM; $n_H = 0.93 \pm 0.04$ and 0.79 ± 0.13; $n = 5$, respectively; Figure 5b) was not significantly different from that of basal GIRK currents in oocytes injected with GIRK1 and GIRK2 mRNAs ($P > 0.05$, $IC_{25}$ and $IC_{50}$ values for each NRI, Student's *t*-test; $P > 0.05$ at each concentration, Tukey–Kramer *post hoc* test), suggesting that the effects of the NRIs on $A_1$R-activated GIRK channels were similar to those on GIRK channels activated by basally free G-protein βγ subunits present in oocytes.

GIRK channels are activated by various G-protein-coupled receptors through the direct action of G-protein βγ subunits released from the heterotrimeric G-protein complex (Dascal, 1997; Kobayashi and Ikeda, 2006). The effects of the NRIs on GIRK channels activated by G-protein-coupled signaling mechanisms were further examined using GTPγS, a nonhydrolyzable GTP analogue that maintains G-proteins in an activated state. Injection of GTPγS into *Xenopus* oocytes injected with GIRK1 and

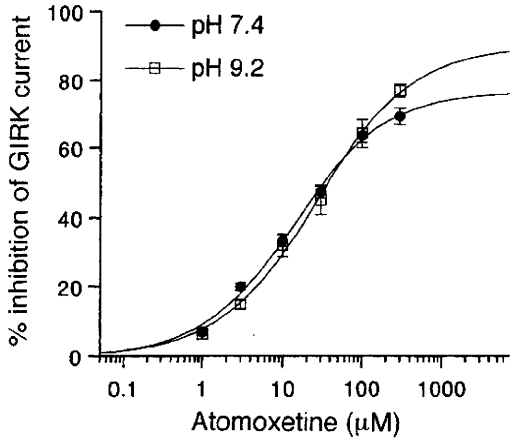


**Figure 4** Concentration–response relationships for inhibition of GIRK channels by atomoxetine at different pH values. The magnitudes of inhibition of GIRK currents by atomoxetine were compared with the 3 mM $Ba^{2+}$-sensitive current components in oocytes expressing GIRK1/2 channels (1021.5 ± 100.8 nA, pH 7.4, $n=8$; 852.4 ± 141.4 nA, pH 9.2, $n=6$). Current responses were measured at a membrane potential of −70 mV in an hK solution containing 96 mM $K^+$. Each point and error bar represents the mean ± SEM of the percentage responses.

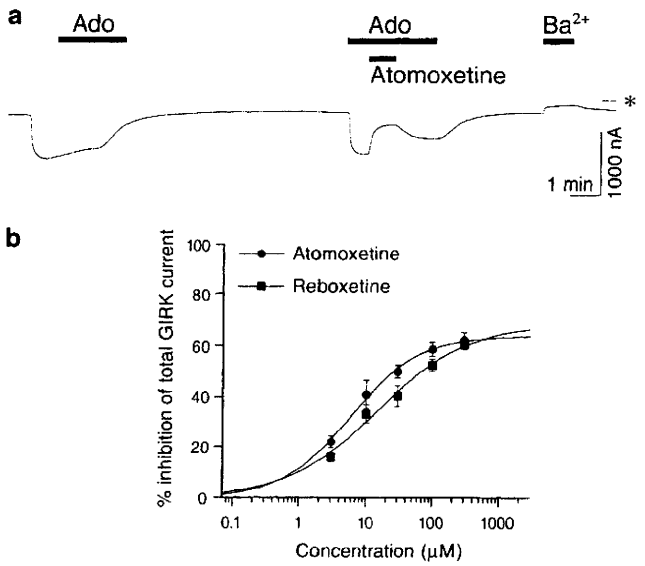


**Figure 5** Effects of atomoxetine and reboxetine on GIRK channels activated by a G-protein-coupled receptor. (a) Current responses to 100 nM adenosine (Ado), 30 μM atomoxetine during application of 100 nM Ado, and 3 mM $Ba^{2+}$ in an oocyte co-injected with mRNAs for GIRK1 and GIRK2 channels and the $A_1$ adenosine receptor ($A_1R$) are shown. Bars show the duration of application. Asterisk indicates the zero current level. (b) Concentration–response relationships for the inhibitory effects of atomoxetine and reboxetine on total GIRK currents composed of Ado-induced GIRK currents and basal GIRK currents. Each point and error bar represents the mean ± SEM of the percentage responses. Current responses were measured at a membrane potential of −70 mV in an hK solution containing 96 mM $K^+$.

GIRK2 mRNAs increased inward currents with time and reached a steady-state level (938.9 ± 119.2 nA, $n=18$) as reported earlier (Kovoor *et al*, 1995). The increased inward currents were completely blocked by 3 mM $Ba^{2+}$, whereas GTPγS injection into uninjected oocytes had no significant effect on current responses to 3 mM $Ba^{2+}$ (3.9 ± 2.1 nA, $n=9$). Increased GIRK currents composed of basal GIRK currents and GTPγS-induced GIRK currents were inhibited by atomoxetine or reboxetine ($IC_{50}=29.0\pm6.2$ and 52.3 ± 10.1 μM; $n_H=1.28\pm0.04$ and $1.14\pm0.06$; $n=6$ and 12, respectively). The percentage inhibition of total GIRK currents by atomoxetine or reboxetine was not significantly different from that of basal GIRK currents in GTPγS-untreated oocytes injected with GIRK1 and GIRK2 mRNAs ($P>0.05$, $IC_{50}$ value for each NRI, Student's *t*-test; $P>0.05$ at each concentration, Tukey–Kramer *post hoc* test), suggesting that the effects of the NRIs on basally active GIRK channels and GIRK channels activated by G-protein activation induced by GTPγS were similar.

## Atomoxetine Inhibits Ethanol-Induced GIRK Currents

GIRK channels are also activated by ethanol independent of G-protein signaling pathways (Kobayashi *et al*, 1999). Atomoxetine was shown to reduce cumulative heavy drinking days in the treatment of psychiatric patients with comorbid alcohol use disorders (Wilens *et al*, 2008). Therefore, we also examined the effects of atomoxetine on GIRK channel activation induced by ethanol. The effects of atomoxetine were evaluated by measuring the amplitude of the ethanol-induced current response during extracellular application of atomoxetine at different concentrations. In oocytes injected with GIRK1 and GIRK2 mRNAs, the GIRK currents induced by 100 mM ethanol (420.0 ± 32.5 nA, $n=5$) were reversibly attenuated in the presence of atomoxetine ($IC_{25}=5.8\pm1.1$ μM; $IC_{50}=15.4\pm3.1$ μM; $n_H=1.22\pm0.22$; $n=5$; Figure 6a and b). However, 100 mM ethanol-induced GIRK currents were not significantly affected by intracellularly applied atomoxetine (104.3 ± 2.8% of untreated control current, paired *t*-test, $P>0.1$, $n=5$; Figure 6c). Moreover, in oocytes expressing GIRK channels, the basal currents were not significantly affected by intracellularly applied atomoxetine (103.0 ± 2.2% of untreated control current, paired *t*-test, $P>0.1$, $n=5$). The results indicate that intracellular atomoxetine could not inhibit GIRK channels. In contrast, GIRK channel inhibition induced by extracellularly applied atomoxetine, which is mainly protonated at pH 7.4, was reversible with washout (Figures 1a and 6a). As the protonated form may not readily permeate the cell membrane, extracellularly applied atomoxetine may exist mainly on the extracellular side. Altogether, extracellular atomoxetine may inhibit GIRK channels activated by ethanol.

## DISCUSSION

In this study, we showed that atomoxetine and structurally related reboxetine, clinically used selective NRIs, inhibited brain-type GIRK1/2 and GIRK2 channels and cardiac-type GIRK1/4 channels expressed in *Xenopus* oocytes. However, Kir1.1 and Kir2.1 channels in other Kir channel subfamilies were insensitive to both NRIs. The inhibitory effects on GIRK channels were concentration-dependent, but voltage-independent, and time-independent during each voltage pulse. The present results suggest that the site of action on

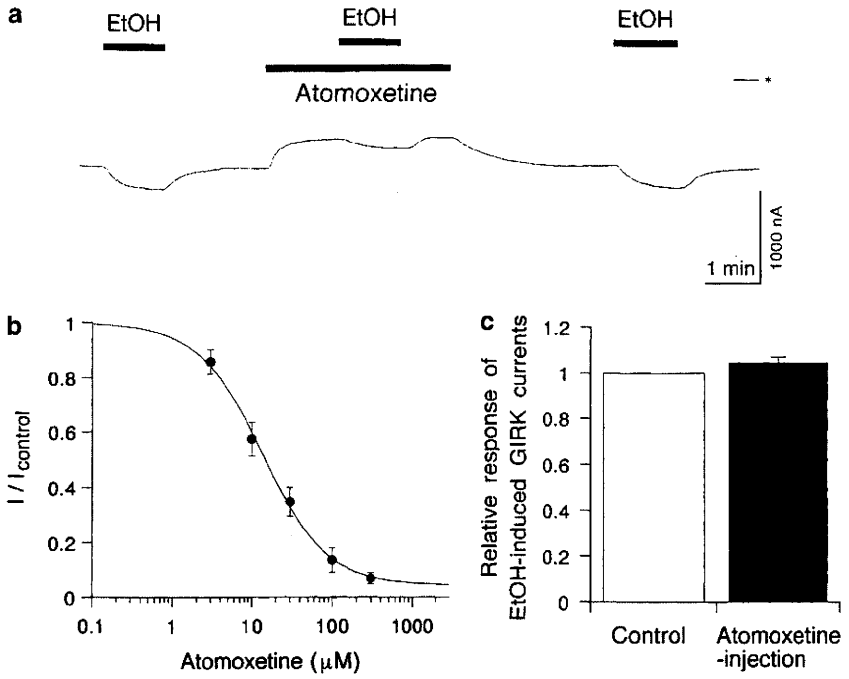


**Figure 6** Effects of atomoxetine on ethanol-induced GIRK currents. (a) Current responses to 100 mM ethanol (EtOH), 100 mM EtOH in the presence of 30 μM atomoxetine, and 100 mM EtOH in an oocyte injected with GIRK1 and GIRK2 mRNAs. Asterisk indicates the zero current level. Bars show the duration of application. (b) Concentration-dependent inhibition of EtOH-induced GIRK currents by atomoxetine. $I_{control}$ is the amplitude of GIRK currents induced by 100 mM EtOH (420.0 ± 32.5 nA, $n = 5$), and $I$ is the current amplitude in the presence of atomoxetine. (c) Lack of effect of intracellular atomoxetine on 100 mM EtOH-induced GIRK currents. The amplitude of EtOH-induced GIRK currents after atomoxetine injection (black bar) was compared with the amplitude of EtOH-induced GIRK currents before the injection (control, white bar) in the same oocyte expressing GIRK channels ($n = 5$). Current responses were measured at a membrane potential of −70 mV in an hK solution containing 96 mM $K^+$. All values are expressed as mean ± SEM.

the channels may be extracellular. In contrast, blockade of GIRK channels by extracellular $Ba^{2+}$ and $Cs^+$, which occlude the pore of the open channel, shows a concentration-dependence, a voltage-dependence, and a time-dependence with a comparatively small effect on the instantaneous current but a marked inhibition of the steady-state current at the end of the voltage pulses (Lesage *et al*, 1995). These observations suggest that atomoxetine and reboxetine may cause an allosteric conformational change in GIRK channels even before the voltage pulses, rather than simple occlusion of the open channel. Interestingly, GIRK channels are also inhibited by the selective serotonin reuptake inhibitor (SSRI) fluoxetine (Kobayashi *et al*, 2003; Takahashi *et al*, 2006), despite a great difference in the pharmacological profiles for monoamine transporters between the two NRIs and fluoxetine. The chemical structures of atomoxetine and reboxetine are related to fluoxetine (Boot *et al*, 2005; Supplementary Figure S1), suggesting that the common moiety of the structures may play a key role in interacting with GIRK channels. Additionally, the *Xenopus* oocyte expression assay with a conventional two-electrode voltage clamp is generally conducted using defolliculated oocytes, which are still covered over the plasma membrane with the vitelline membrane, at room temperature (Fraser and Djamgoz, 1992; Weber, 1999; Ikeda *et al*, 2003). Further studies using mammalian cells, including neurons and cardiac myocytes, at physiological temperature may be useful for advancing our understanding of the effects of NRIs on GIRK channels.

Atomoxetine is predominantly metabolized by the genetically polymorphic cytochrome P450 2D6 (CYP2D6) pathway, and its pharmacokinetics and metabolism are characterized by two distinct activities of CYP2D6: active or poor metabolic capability (Witcher *et al*, 2003; Simpson and Plosker, 2004). The maximum plasma concentrations during treatment with atomoxetine at therapeutic doses ranged from ~0.7–4.8 μM in CYP2D6 active metabolizers (Witcher *et al*, 2003), whereas those in CYP2D6 poor metabolizers (~7% of the Caucasian population) were six-fold higher than those in CYP2D6 active metabolizers (Simpson and Plosker, 2004). Additionally, co-administration of the SSRI paroxetine, a potent inhibitor of CYP2D6, increased the plasma concentrations of atomoxetine by 3.5-fold, with a pharmacokinetic profile similar to CYP2D6 poor metabolizers (Belle *et al*, 2002), suggesting a significant increase in atomoxetine concentrations with concomitant treatment with CYP2D6 inhibitors. The maximum plasma concentrations of reboxetine at therapeutic doses in depressed patients ranged from 0.5 to 2.1 μM (Poggesi *et al*, 2000). Additionally, increases in doses of the NRIs are associated with increases in plasma concentrations (Öhman *et al*, 2001; Witcher *et al*, 2003), and the concentration in a fatal case of atomoxetine overdose was reported to be up to 32.5 μM (Garside *et al*, 2006). Recent studies using radiolabeled NRI ligands have indicated that NRIs are extensively distributed in most tissues (Kiyono *et al*, 2004, 2008; Kanegawa *et al*, 2006). Indeed, brain and heart levels of NRIs were ~4.7- to 6.5-fold and 9- to 12-fold higher for

atomoxetine (Kiyono *et al*, 2004) and ~15- to 16-fold and 21- to 32-fold higher for reboxetine than corresponding blood levels, respectively (Kanegawa *et al*, 2006; Kiyono *et al*, 2008). Therefore, brain and heart concentrations during treatment with therapeutic doses of atomoxetine and reboxetine, as well as after overdose, overlap with their effective concentrations in inhibiting brain- and cardiac-type GIRK channels (Figure 2). GIRK channels in the brain and heart may be inhibited by atomoxetine and reboxetine, particularly with the use of atomoxetine with CYP2D6 poor metabolizers or co-administration of CYP2D6 inhibitors. Inhibition of GIRK channels causes a depolarization of membrane potential, resulting in an increase in cell excitability (Kuzhikandathil and Oxford, 2002). GIRK channels have an important function in regulating neuronal excitability, synaptic transmission, and heart rate (Lüscher *et al*, 1997; Kovoor *et al*, 2001). Therefore, even partial inhibition of GIRK channels by atomoxetine and reboxetine may affect certain brain and heart functions.

Interestingly, GIRK2 knockout mice exhibit reduced anxiety-related behavior (Blednov *et al*, 2001). In clinical studies, reboxetine and atomoxetine were effective in the treatment of panic disorder and comorbid anxiety disorder, respectively (Versiani *et al*, 2002; Geller *et al*, 2007), suggesting their anxiolytic properties. Although their therapeutic effects are generally thought to be primarily attributable to inhibition of norepinephrine reuptake in the brain (Hajós *et al*, 2004; Simpson and Plosker, 2004), inhibition of GIRK channels may also contribute to improvement of anxiety symptoms.

GIRK2 knockout mice exhibit spontaneous seizures and are more susceptible to seizures induced by pentylenetetrazol than wild-type mice (Signorini *et al*, 1997). In animal studies using atomoxetine or reboxetine, convulsions were observed only at extremely high doses (Wong *et al*, 2000; Wernicke *et al*, 2007). The incidence of seizures during treatment with NRIs has been reportedly rare (Montgomery, 2005; Wernicke *et al*, 2007). Brain levels of the drugs in overdose cases may be considerably higher than levels during treatment at therapeutic doses (Poggesi *et al*, 2000; Kiyono *et al*, 2004, 2008; Garside *et al*, 2006; Kanegawa *et al*, 2006), suggesting that potent inhibition of neuronal GIRK channels by atomoxetine and reboxetine after overdose may contribute to increased seizure activity. However, the NRIs simultaneously increase extracellular levels of norepinephrine in the brain (Hajós *et al*, 2004; Simpson and Plosker, 2004), and norepinephrine has anticonvulsant effects (Ahern *et al*, 2006). The enhancement of norepinephrine by NRIs may be involved in the rare incidence of seizures. Although atomoxetine and reboxetine are generally well tolerated and have a benign side effect profile (Hajós *et al*, 2004; Simpson and Plosker, 2004), the inhibitory effects on GIRK channels may be partly related to the occurrence of other neurological side effects, such as insomnia and dizziness.

In the heart, GIRK channels cause slowing of heart rate in response to activation of $M_2$ muscarinic receptors through acetylcholine release from the stimulated vagus nerve (Kubo *et al*, 1993b; Krapivinsky *et al*, 1995). GIRK1 or GIRK4 knockout mice exhibit slightly elevated resting heart rates (Bettahi *et al*, 2002). Atomoxetine and reboxetine are associated with modest increases in heart rate (Hajós *et al*, 2004; Simpson and Plosker, 2004) and tachycardia in cases of toxicity (LoVecchio and Kashani, 2006). The binding affinities of atomoxetine and reboxetine for the muscarinic receptor are in the low micromolar range (Cusack *et al*, 1994; Wong *et al*, 2000; Hajós *et al*, 2004). Inhibition of norepinephrine reuptake enhances sympathetic nerve activity (Keller *et al*, 2004). The present results indicate that atomoxetine and reboxetine inhibit cardiac-type GIRK1/4 channels at clinically relevant heart concentrations. Altogether, an increase in heart rate during treatment with the drugs may be related to not only enhancement of sympathetic nerve activity and antagonism of the muscarinic receptor but also inhibition of atrial GIRK channels. Additionally, QT interval prolongation in two cases with atomoxetine overdose was reported (Barker *et al*, 2004; Sawant and Daviss, 2004). Recently, atomoxetine at micromolar concentrations was shown to inhibit cloned human *ether-a-go-go*-related gene (hERG) channels underlying rapidly activating delayed rectifier $K^+$ currents using the *Xenopus* oocyte expression assay (Scherer *et al*, 2009). Inhibition of delayed rectifier $K^+$ currents induces QT prolongation (Scherer *et al*, 2009), and QT prolongation after atomoxetine overdose may be related to inhibition of hERG channels but not GIRK channels among cardiac $K^+$ channels. Furthermore, GIRK4 knockout mice are resistant to atrial fibrillation caused by vagal stimulation without showing any changes in atrioventricular nodal function and ventricular arrhythmias (Kovoor *et al*, 2001). Tertiapine, a selective GIRK blocker in the heart, terminates atrial fibrillation, the most common arrhythmia (Hashimoto *et al*, 2006). Atomoxetine and reboxetine may therefore have an advantage in treating psychiatric patients with comorbid atrial fibrillation.

Atomoxetine was shown to reduce cumulative heavy drinking days in the treatment of psychiatric patients with comorbid alcohol use disorders (Wilens *et al*, 2008). Interestingly, GIRK2 knockout mice show reduced ethanol-induced conditioned taste aversion and conditioned place preference and are less sensitive than wild-type mice to some of the acute effects of ethanol, including anxiolysis, habituated locomotor stimulation, and acute handling-induced convulsions (Hill *et al*, 2003). In the present study, atomoxetine inhibited ethanol-induced GIRK1/2 currents, suggesting that it may suppress some GIRK-related effects of ethanol. Furthermore, GIRK knockout mice also show reduced cocaine self-administration (Morgan *et al*, 2003) and attenuation of the morphine withdrawal syndrome (Cruz *et al*, 2008). In the nervous system, GIRK channels are activated by $\mu$-opioid and $CB_1$ cannabinoid receptors (North, 1989; Dascal, 1997; Kobayashi and Ikeda, 2006). Reboxetine and atomoxetine have also been shown to be useful in the treatment of cocaine dependence and marijuana users, respectively (Tirado *et al*, 2008; Szerman *et al*, 2005). Inhibition of GIRK channels by atomoxetine and reboxetine may have a role in the treatment of drug addiction.

## ACKNOWLEDGEMENTS

We are grateful to Dr Kansaku Baba for his cooperation and Mr Kazuo Kobayashi (Niigata University) for his assistance.

We also thank Dr Steven C Hebert and Dr Lily Y Jan for generously providing the Kir1.1 cDNA and Kir2.1 cDNA, respectively. This work was supported by research grants from the Ministry of Education, Science, Sports, and Culture of Japan and from the Ministry of Health, Labour, and Welfare of Japan.

## DISCLOSURE

The authors declare that over the past 3 years Kazutaka Ikeda has received research grants or expenses that are not related to this study from Fujifilm Corporation, the Mitsubishi Foundation, the Naito Foundation, and the Smoking Science Foundation, and a lecture fee from Dainippon Sumitomo Pharma and Kyowa Hakko Kirin. The authors declare that, except for income received from their primary employer and the aforementioned disclosures, no financial support or compensation has been received from any individual or corporate entity over the past 3 years for research or professional service, and there are no personal financial holdings that could be perceived as constituting a potential conflict of interest.

## REFERENCES

Ahern TH, Javors MA, Eagles DA, Martillotti J, Mitchell HA, Liles LC *et al* (2006). The effects of chronic norepinephrine transporter inactivation on seizure susceptibility in mice. *Neuropsychopharmacology* **31**: 730–738.

Barker MJ, Benitez JG, Ternullo S, Juhl GA (2004). Acute oxcarbazepine and atomoxetine overdose with quetiapine. *Vet Hum Toxicol* **46**: 130–132.

Belle DJ, Ernest CS, Sauer JM, Smith BP, Thomasson HR, Witcher JW (2002). Effect of potent CYP2D6 inhibition by paroxetine on atomoxetine pharmacokinetics. *J Clin Pharmacol* **42**: 1219–1227.

Bettahi I, Marker CL, Roman MI, Wickman K (2002). Contribution of the Kir3.1 subunit to the muscarinic-gated atrial potassium channel IKACh. *J Biol Chem* **277**: 48282–48288.

Blednov YA, Stoffel M, Chang SR, Harris RA (2001). Potassium channels as targets for ethanol: studies of G-protein-coupled inwardly rectifying potassium channel 2 (GIRK2) null mutant mice. *J Pharmacol Exp Ther* **298**: 521–530.

Boot J, Cases M, Clark BP, Findlay J, Gallagher PT, Hayhurst L *et al* (2005). Discovery and structure-activity relationships of novel selective norepinephrine and dual serotonin/norepinephrine reuptake inhibitors. *Bioorg Med Chem Lett* **15**: 699–703.

Cruz HG, Berton F, Sollini M, Blanchet C, Pravetoni M, Wickman K *et al* (2008). Absence and rescue of morphine withdrawal in KIR/Kir3 knock-out mice. *J Neurosci* **28**: 4069–4077.

Cusack B, Nelson A, Richelson E (1994). Binding of antidepressants to human brain receptors: focus on newer generation compounds. *Psychopharmacology* **114**: 559–565.

Dascal N (1997). Signalling via the G protein-activated $K^+$ channels. *Cell Signal* **9**: 551–573.

Fraser SP, Djamgoz MBA (1992). *Xenopus* oocytes: endogenous electrophysiological characteristics. In: Osborne NN (ed). *Current Aspects of the Neurosciences*, Vol 4. Macmillan: London. pp 267–315.

Garland M, Kirkpatrick P (2004). Atomoxetine hydrochloride. *Nat Rev Drug Discovery* **3**: 385–386.

Garside D, Ropero-Miller JD, Riemer EC (2006). Postmortem tissue distribution of atomoxetine following fatal and nonfatal doses: three case reports. *J Forensic Sci* **51**: 179–182.

Geller D, Donnelly C, Lopez F, Rubin R, Newcorn J, Sutton V *et al* (2007). Atomoxetine treatment for pediatric patients with attention-deficit/hyperactivity disorder with comorbid anxiety disorder. *J Am Acad Child Adolesc Psychiatry* **46**: 1119–1127.

Hajós M, Fleishaker JC, Filipiak-Reisner JK, Brown MT, Wong EHF (2004). The selective norepinephrine reuptake inhibitor antidepressant reboxetine: pharmacological and clinical profile. *CNS Drug Rev* **10**: 23–44.

Hashimoto N, Yamashita T, Tsuruzoe N (2006). Tertiapine, a selective $IK_{ACh}$ blocker, terminates atrial fibrillation with selective atrial effective refractory period prolongation. *Pharmacol Res* **54**: 136–141.

Hill KG, Alva H, Blednov YA, Cunningham CL (2003). Reduced ethanol-induced conditioned taste aversion and conditioned place preference in GIRK2 null mutant mice. *Psychopharmacology* **169**: 108–114.

Ho K, Nichols CG, Lederer WJ, Lytton J, Vassilev PM, Kanazirska MV *et al* (1993). Cloning and expression of an inwardly rectifying ATP-regulated potassium channel. *Nature* **362**: 31–38.

Ikeda K, Yoshii M, Sora I, Kobayashi T (2003). Opioid receptor coupling to GIRK channels: *in vitro* studies using a *Xenopus* oocyte expression system and *in vivo* studies on weaver mutant mice. *Methods Mol Med* **84**: 53–64.

Inanobe A, Yoshimoto Y, Horio Y, Morishige K-I, Hibino H, Matsumoto S *et al* (1999). Characterization of G-protein-gated $K^+$ channels composed of Kir3.2 subunits in dopaminergic neurons of the substantia nigra. *J Neurosci* **19**: 1006–1017.

Kadhe NG, Chillar AJ, Deshmukh YA (2003). Reboxetine: a novel antidepressant. *J Postgrad Med* **49**: 373–375.

Kanegawa N, Kiyono Y, Kimura H, Sugita T, Kajiyama S, Kawashima H *et al* (2006). Synthesis and evaluation of radioiodinated (S,S)-2-(α-(2-iodophenoxy)benzyl)morpholine for imaging brain norepinephrine transporter. *Eur J Nucl Med Mol Imaging* **33**: 639–647.

Karschin C, Dißmann E, Stuhmer W, Karschin A (1996). IRK(1-3) and GIRK(1-4) inwardly rectifying $K^+$ channel mRNAs are differentially expressed in the adult rat brain. *J Neurosci* **16**: 3559–3570.

Keller NR, Diedrich A, Appalsamy M, Tuntrkool S, Lonce S, Finney C *et al* (2004). Norepinephrine transporter-deficient mice exhibit excessive tachycardia and elevated blood pressure with wakefulness and activity. *Circulation* **110**: 1191–1196.

Kiyono Y, Kanegawa N, Kawashima H, Kitamura Y, Iida Y, Saji H (2004). Evaluation of radioiodinated (R)-*N*-methyl-3-(2-iodophenoxy)-3-phenylpropanamine as a ligand for brain norepinephrine transporter imaging. *Nucl Med Biol* **31**: 147–153.

Kiyono Y, Sugita T, Ueda M, Kawashima H, Kanegawa N, Kuge Y *et al* (2008). Evaluation of radioiodinated (2S,αS)-2-(α-(2-iodophenoxy)benzyl)morpholine as a radioligand for imaging of norepinephrine transporter in the heart. *Nucl Med Biol* **35**: 213–218.

Kobayashi T, Ikeda K (2006). G protein-activated inwardly rectifying potassium channels as potential therapeutic targets. *Curr Pharm Des* **12**: 4513–4523.

Kobayashi T, Ikeda K, Ichikawa T, Abe S, Togashi S, Kumanishi T (1995). Molecular cloning of a mouse G-protein-activated $K^+$ channel (mGIRK1) and distinct distributions of three GIRK (GIRK1, 2 and 3) mRNAs in mouse brain. *Biochem Biophys Res Commun* **208**: 1166–1173.

Kobayashi T, Ikeda K, Kojima H, Niki H, Yano R, Yoshioka T *et al* (1999). Ethanol opens G-protein-activated inwardly rectifying $K^+$ channels. *Nat Neurosci* **2**: 1091–1097.

Kobayashi T, Ikeda K, Kumanishi T (2000). Inhibition by various antipsychotic drugs of the G-protein-activated inwardly rectifying $K^+$ (GIRK) channels expressed in *Xenopus* oocytes. *Br J Pharmacol* **129**: 1716–1722.

Kobayashi T, Ikeda K, Kumanishi T (2002). Functional characterization of an endogenous *Xenopus* oocyte adenosine receptor. *Br J Pharmacol* **135**: 313–322.